Received: 14 September 2020 | Revised: 24 November 2020 | Accepted: 24 November 2020

DOI: 10.1002/cne.25077

RESEARCH ARTICLE

JCN RESEARCH IN SYSTEMS NEUROSCIENCE THE JOURNAL OF COMPARATIVE NEUROLOGY WILEY

Johnston's organ and its central projections in *Cataglyphis* desert ants

Robin Grob[1] | Clara Tritscher[1] | Kornelia Grübel[1] | Christian Stigloher[2] | Claudia Groh[1] | Pauline N. Fleischmann[1] | Wolfgang Rössler[1]

[1]Behavioral Physiology and Sociobiology (Zoology II), Biocenter, University of Würzburg, Würzburg, Germany

[2]Imaging Core Facility, Biocenter, University of Würzburg, Würzburg, Germany

Correspondence
Robin Grob, Behavioral Physiology and Sociobiology (Zoology II), Biocenter, University of Würzburg, Würzburg, Germany.
Email: robin.grob@uni-wuerzburg.de

Funding information
Deutsche Forschungsgemeinschaft, Grant/Award Numbers: FL1060/1-1, INST 93/829-1, Ro1177/7-1; Klaus Tschira Stiftung, Grant/Award Number: GSO/KT 16

Abstract

The Johnston's organ (JO) in the insect antenna is a multisensory organ involved in several navigational tasks including wind-compass orientation, flight control, graviception, and, possibly, magnetoreception. Here we investigate the three dimensional anatomy of the JO and its neuronal projections into the brain of the desert ant *Cataglyphis*, a marvelous long-distance navigator. The JO of *C. nodus* workers consists of 40 scolopidia comprising three sensory neurons each. The numbers of scolopidia slightly vary between different sexes (female/male) and castes (worker/queen). Individual scolopidia attach to the intersegmental membrane between pedicel and flagellum of the antenna and line up in a ring-like organization. Three JO nerves project along the two antennal nerve branches into the brain. Anterograde double staining of the antennal afferents revealed that JO receptor neurons project to several distinct neuropils in the central brain. The T5 tract projects into the antennal mechanosensory and motor center (AMMC), while the T6 tract bypasses the AMMC via the saddle and forms collaterals terminating in the posterior slope (PS) (T6I), the ventral complex (T6II), and the ventrolateral protocerebrum (T6III). Double labeling of JO and ocellar afferents revealed that input from the JO and visual information from the ocelli converge in tight apposition in the PS. The general JO anatomy and its central projection patterns resemble situations in honeybees and *Drosophila*. The multisensory nature of the JO together with its projections to multisensory neuropils in the ant brain likely serves synchronization and calibration of different sensory modalities during the ontogeny of navigation in *Cataglyphis*.

KEYWORDS
ant brain, chordotonal organ, graviception, magnetic compass, multisensory integration, navigation, wind compass

1 | INTRODUCTION

Johnston's organ (JO) is a highly elaborated multisensory organ in the insect antenna. Being present in most insects, the JO shows a wide range in structural organization (Child, 1894; McIver, 1985). For example in flies the JO comprises ~720 sensory neurons in *Drosophila melanogaster* (Kamikouchi, Shimada, & Ito, 2006), but it may contain as many as 30,000 sensory neurons in mosquitos (Boo &

Richards, 1975). This diversity is connected to a multitude of functions (Child, 1894; McIver, 1985). The JO is known as a chordotonal organ, a mechanoreceptive organ sensitive to the slightest antennal movements (review: Yack, 2004). The antennal deflections may be caused by gravitational or wind forces (review: McIver, 1985). Therefore, the JO is involved in graviception (Kamikouchi et al., 2009; Vowles, 1954), flight control, and the detection of wind directions (Sane, Dieudonné, Willis, & Daniel, 2007). Johnston himself classified the JO as an auditory apparatus in *Culex* mosquitoes (Johnston, 1855). In the fruit fly *D. melanogaster* (Göpfert & Robert, 2001a; Göpfert & Robert, 2002) and the mosquito *Aedes aegypti* (Cator, Arthur, Harrington, & Hoy, 2009), the JO detects airborne sounds, for example, during courtship. In the honeybee *Apis mellifera*, the JO plays a role in detecting airborne and vibrational sounds produced during the waggle dance, a form of communication that informs nestmates about the distance and direction of food sources (Dreller & Kirchner, 1993a; Dreller & Kirchner, 1993b; Dreller & Kirchner, 1995).

The peripheral morphology of the JO in the antenna has been studied in detail in Diptera (e.g., fruitflies: Göpfert & Robert, 2002; mosquitos: Johnston, 1855), in Hymenoptera (e.g., Child, 1894; bees: Ai, Nishino, & Itoh, 2007; Dreller & Kirchner, 1995; sawflies: Hallberg, 1981; ants: Masson & Gabouriaut, 1973; Vowles, 1954), and many other insect species (e.g., Snodgrass, 1926). The sensory structures are located at the joint of the pedicel and the flagellum (Figure 1a) and attached to the intersegmental membrane. The JO consists of a species-specific number of mechanosensory complexes, so-called scolopidia. Individual scolopidia usually comprise four different cell types: (1) between one to four sensory neurons, (2) scolopale cells that ensheath the dendrites of the sensory neurons, (3) cap cells, and (4) glial cells—sometimes also referred to as supporting cells (review: Yack, 2004). Via the cap cells, the scolopidia attach to the intersegmental membrane by chitin caps. These attachment sites can be observed as pits on the outside of the pedicel's most distal end (Snodgrass, 1926). The caps are connected to scolopale rods within the scolopale cells, and the mechanosensitive portions of the dendrites are suspended within the rods (Todi, Sharma, & Eberl, 2004).

To detect antennal movement, Todi et al. (2004) suggested a "bow and string" mechanism for the function of the JO: Antennal movement deflects the intersegmental membrane between pedicel and flagellum. This force is transduced via the cap cells to the scolopale cells and the dendrites, on which mechanosensitive ion channels are opened. The resulting action potentials are transmitted along the JO afferent projections into the central brain (Todi et al., 2004).

Although the morphology of the JO has been studied in various insect species, the afferent projections of the JO came into focus in only a limited number of species. In the honeybee, mechanosensory

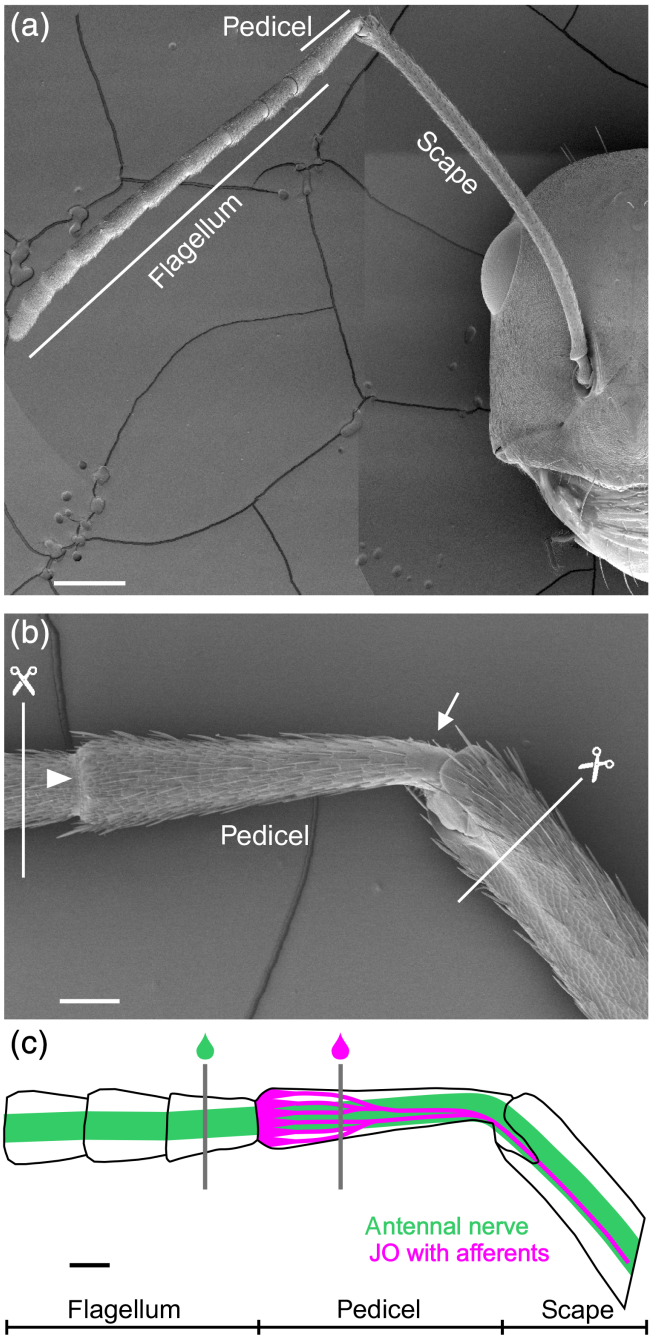

FIGURE 1 The *Cataglyphis nodus* antenna. (a) Scanning electron microscopy image of the ant's (*C. nodus* worker) head with the antenna. The antenna is divided into three parts: The flagellum is located most distally from the head. It comprises 10 flagellomeres. The middle part is the pedicel, which houses mechanosensory organs, particularly the Johnston's organ (JO). The scape is connected to the head capsule. Scale bar 500 μm. (b) Close up of the pedicel of a *C. nodus* worker. At the joint between flagellum and pedicel, dents in the cuticle indicate the attachment sites of the JO to the intersegmental membrane (arrowhead). A hair plate is located close to the joint of pedicel and scape (arrow). For serial sectioning, the antenna was cut (scissors symbols) at the first flagellomere and at an equivalent distance from the pedicel at the scape before fixation. Scale bar 100 μm. (c) Scheme of the anterograde double staining procedure. The antenna was first cut at the first flagellomere and dye was applied (green droplet). After 3 h, the antenna was cut at the level of the pedicel to apply a second dye (magenta droplet). This technique allowed for a differential staining of the antennal nerve without afferents of the JO (green) and with afferents of the JO (magenta). Scale bar 100 μm

information from the antennae projects into the antennal mechanosensory and motor center (AMMC) (e.g., Maronde, 1991). In both the honeybee and *Drosophila* sensory afferents of the JO project along the antennal nerve (AN) into the AMMC (Ai et al., 2007; Brockmann & Robinson, 2007; Kamikouchi et al., 2006). In *D. melanogaster*, different sensory modalities—like sound and wind—activate different populations of JO neurons. These innervate distinct areas within the AMMC (Yorozu et al., 2009). This enables the JO to function as an efficient multisensory organ that distinguishes between different sensory modalities and qualities. Additionally, the JO afferents project into the ventral region of the ventrolateral protocerebrum, and the posterior part of the subesophageal ganglion (*A. mellifera*: Ai et al., 2007; *D. melanogaster*: Kamikouchi et al., 2006). Interestingly, JO afferents terminate in similar brain areas like projections from visual input regions, that is, the compound eyes and the ocelli (Ai et al., 2007; Maronde, 1991; Okubo, Patella, D'Alessandro, & Wilson, 2020). The integration of compass information from both visual and JO input likely is important for successful multimodal navigation, especially in challenging habitats (Okubo et al., 2020).

Despite the fact that ants are highly tactile insects, surprisingly little research has been done on the fine structure of the JO in ants (*Camponotus vagus*: Masson & Gabouriaut, 1973; *Formica rufa*: Vowles, 1954), and none on the central projections of JO receptor neurons. One major difference between especially flies and ants is that the latter are not able to perceive airborne sound (Roces & Tautz, 2001). This, however, provides a unique opportunity to study the involvement of the JO in other sensory modalities than hearing.

Cataglyphis desert ants have been favorable experimental models for sensory orientation for decades, mainly because of their astonishing navigational capabilities and the involved sophisticated navigational tool kit (review: Wehner, 2003, 2020). *Cataglyphis* is intensively studied for the use of polarized skylight as directional information for path integration during homing back to their nest after far ranging food searches. Many of their navigational tools, like the skylight compass or panoramic landmark orientation, are based on vision and, therefore, the ants' eyes. However, for several navigational components the location of the sensory organ is still unknown or remained speculative: During early learning walks, *Cataglyphis nodus* uses the earth's magnetic field as a compass (Fleischmann, Grob, Müller, Wehner, & Rössler, 2018). Later, during foraging, *Cataglyphis* ants use gravitational information to account for slopes during path integration along uneven terrain (Ronacher, 2020; Wohlgemuth, Ronacher, & Wehner, 2001). To finally pinpoint food sources on their extensive foraging trips or the nest entrance in the final approach during homing, *Cataglyphis fortis* also utilizes a wind compass (Steck, Hansson, & Knaden, 2009; Wolf & Wehner, 2000). Especially for the latter two, the JO is a promising candidate for the responsible sensory organ, which already received support from experiments including antennal manipulations (Wolf & Wehner, 2000). As an interesting further aspect, in contrast to the ambulatory worker caste, the sexual castes of *Cataglyphis* (queens and males) are capable of flight (Peeters & Aron, 2017) and therefore require additional sensory machinery for flight stabilization. Surprisingly, until now the JO in the antenna of *Cataglyphis* ants had not been investigated in detail. In this study, we analyze the three dimensional structure of the JO in the antenna of *C. nodus* together with the central projections of its sensory afferents into the ant brain. Additionally, we compare the JO in young *C. nodus* queens and males with the JO in workers. This together provides first insight toward understanding the role of the antennae, particularly the JO, in providing various sensory channels feeding into brain neuropils potentially involved in navigational tasks in desert ants.

2 | MATERIAL AND METHODS

For the experiments, colonies of *Cataglyphis nodus* (Brullé 1832) were excavated in the pine forests of Schinias national park (38.153783, 24.030913) and Strofylia national park (38.155199, 21. 376582) in Greece during the summers of 2016 and 2019, and subsequently maintained in our ant facility at Zoology II, University of Würzburg. The colonies were housed in a climate chamber (ThermoTec Weilburg GmbH & Co. KG, Weilburg, Germany) at 29°C and 40% humidity. Nest boxes were placed in a dark cabinet that was connected to a foraging arena that offered a 12 h light 12 h dark circle. Adult workers were collected from these colonies in Würzburg. Virgin young queens and males were collected directly from ant colonies in Greece and transported to Würzburg. Ants were anesthetized on ice prior to the experiments.

2.1 | Scanning electron microscopy

For obtaining high-resolution images of the ant antennae, ants were cold-anesthetized and decapitated. Heads of workers, virgin queens, and males were fixated overnight in 6.25% glutaraldehyde in 50 mM phosphate buffer solution (pH 7.4) at 4°C on a shaker. The fixated heads were then rinsed five times for 5 min each in Sørensen phosphate buffer (pH 7.4) (Sörensen, 1912) before being dehydrated in an increasing acetone serial dilution in distilled water at 4°C on a shaker. The dehydration steps were: 15 min in 30%, 20 min in 50%, 30 min in 75%, 45 min in 90%, and twice for 30 min in 100% acetone in water solution. The ant heads were then placed inside a Critical Point Dryer (BAL-TEC CPD 030, BAL-TEC AG, Balzers, Liechtenstein) filled with 100% acetone and dried using CO_2. After dehydration, the heads were sputtered with gold–palladium using a Sputter Coater (BAL-TEC SCD 005, BAL-TEC AG, Balzers, Liechtenstein). The antennae and heads were scanned using a field emission scanning electron microscope (JSM-7500F, JEOL Ltd., Akishima, Japan).

2.2 | Sectioning and 3D reconstruction of the JO

We prepared serial sections of the pedicel to analyze the detailed structure of the JO in *C. nodus*. Decapitated ant heads of workers, virgin queens, and males were fixated in wax, and the antennae were cut in the middle of the first flagellomere behind the pedicel and at equal distance from the pedicel at the scape (Figure 1b). For further preparation, the pedicels were placed in small baskets with a glass fiber

mesh (MN 85/70–403007, Macherey-Nagel GmbH & Co. KG, Düren, Germany) at the bottom. After dissection, the pedicels were immediately fixated in ice-cold 1.5% formaldehyde, 1.5% glutaraldehyde in 0.1 M cacodylate buffer (pH 7.7) with 0.04% $CaCl_2$ on a shaker overnight at 4°C. Subsequently, the antennal parts were rinsed with 30% ethanol in water solution and then dehydrated in an increasing ethanol serial dilution for 30 min in each step: 50%, 70%, 90%, 95%, and twice in 100% ethanol in water solution. The pedicels were cleared twice for 10 min in propylene oxide. Each pedicel was subsequently embedded in Epon 812 (Epon 812, SERVA Electrophoresis GmbH, Heidelberg, Germany) by using an Epon 812 in propylene oxide serial dilution for at least 4 h in each step: 25%, 50%, 75%, and 100% Epon 812 in propylene oxide solution. Subsequently, the pedicels were mounted in 100% Epon 812 in small silicon molds and heated at 60°C for 72 h.

For light microscopy, the embedded pedicels were cut in serial sections of 1.5 μm (cross sections) or 1.4 μm (longitudinal sections) thickness using an ultramicrotome (Leica EM UC7, Leica Microsystems GmbH, Wetzlar, Germany) and stained for contrast using 1% azure II, 1% methylene blue, and 1% borax in water for 1–2 min at 60°C. The stained serial sections were then mounted using Epon 812 on glass slides, covered with a thin coverslip (Cover Slips, Thickness 0, Thermo Fisher Scientific Inc., Waltham, Massachusetts, USA) and hardened for 24 h at 60°C.

The serial sections were imaged using a light microscope (Axiophot, Carl Zeiss Microscopy GmbH, Jena, Germany) equipped with a digital camera (VisiCAM-100, Visitron Systems GmbH, Puchheim, Germany) using VisiView 2.1.4 (Visitron Systems GmbH, Puchheim, Germany). The images from serial sections were aligned using the TrackEM2 (Cardona et al., 2012) plugin for ImageJ 1.52n (Wayne Rasband, National Institutes of Health, USA) and 3D reconstructed in Amira (Amira-Avizo Software 2019.1, Thermo Fisher Scientific Inc., Waltham, Massachusetts, USA).

2.3 | Anterograde tracings of JO afferents and 3D reconstruction

To label the afferents of sensory neurons of the JO in the pedicel of *C. nodus*, a double anterograde staining procedure was performed using a combination of techniques previously applied in the honeybee (e.g., double staining (Kirschner et al., 2006) and bilateral staining (Ai et al., 2007)) and *Cataglyphis* (Habenstein, Amini, Grübel, el Jundi, & Rössler, 2020). The head of cold-anesthetized ants was fixed with dental wax. The antenna was cut at the first flagellomere and a Dextran, Alexa Fluor 488 (D22910, Life Technologies GmbH, Darmstadt, Germany) droplet was placed on the cut end of the antennal nerves (Figure 1c). During incubation for 3–4 h at room temperature in a dark box with high humidity, the dye was allowed to be transported along the antennal nerve branches into the ant's brain. Subsequently, the antenna was cut further proximally at the pedicel and a dextran tetramethylrhodamine droplet (micro-Ruby, D-7162, Life Technologies GmbH, Darmstadt, Germany) was placed on the cut end (Figure 1c). This allowed for specific staining of the central projections of the JO afferents, since projections of the more distal antennae were already stained with Dextran, Alexa Fluor 488, and farther proximal projections (e.g. from the bristle fields at the base of the pedicel) remained excluded. The dye was again incubated for 3–4 h at room temperature in a dark box with high humidity. Afterwards, a small window was cut into the head capsule of the ants to dissect the brain under cooled ant ringer solution (127 mM NaCl, 7 mM KCl, 1.5 mM $CaCl_2$, 0.8 mM Na_2HPO_4, 0.4 mM KH_2PO_4, 4.8 mM TES, and 3.2 mM trehalose, pH 7.0). The brains were fixated overnight in 4% formaldehyde in phosphate-buffered saline (PBS) solution. Afterwards, the brains were rinsed three times for 10 min in PBS and dehydrated using an ethanol in water serial dilution with 10 min in each step: 30%, 50%, 70%, 90%, and twice in 100% ethanol. The dehydrated brains were then cleared in methyl salicylate (4529.1, Carl Roth Gmbh & Co. Kg, Karlsruhe, Germany). This technique stained specifically for the JO afferents with the second tracer. Other, non-JO afferents from the antennae will be labeled with both tracers. Since the first tracer, however, is applied earlier to the afferents from the flagellum, it will have twice the time to be transported. Thus, the staining with the first tracer (green) will appear more prominently in the merged images.

To trace the projections of the complete antennal nerve labeled at the level of the pedicel in distinct neuropils of the ant brain and compare them with double stained preparations (see above), we used combined immunostaining with anti-synapsin antibodies. The antenna was cut at the pedicel and stained with Dextran tetramethylrhodamine only. Subsequently, the brains were dissected and fixated overnight at 4°C in a 4% formaldehyde in water solution. The next day, the brains were rinsed three times for 10 min each in PBS before being rinsed once in 2% Triton-X 100 solution in PBS and twice in 0.5% Triton-X 100 solution in PBS, for 10 min each, to permeabilize cell membranes for antibody application on whole mount brains. The brains were subsequently incubated for 1 h at room temperature on a shaker in a 0.5% Triton-X 100 in PBS with 2% of Normal Goat Serum (NGS, Jackson ImmunoResearch Laboratories, West Grove, USA) solution to block unspecific binding sites. To label synapse-rich neuropils, the brains were then incubated for 3 days at 4°C on a shaker with the primary anti-synapsin antibody from mouse (SYNORF1, kindly provided by E. Buchner, University of Würzburg, Germany) in a 2% antibody with 2% NGS and 0.5% Triton-X 100 in PBS solution. After rinsing the brains five times in PBS for 10 min each, the brains were incubated with the secondary antibody, an anti-mouse antibody from goat with a CF633 dye (Biotium, Hayward, USA) in a 0.4% antibody in PBS with 1% NGS solution, for 2 days at 4°C on a shaker. Afterward, brains were rinsed five times in PBS (10 min each) and dehydrated as described above before clearing in methyl salicylate.

To visualize afferent projections from both the ocelli and the JO, double stained differential tracings were carried out. Anterograde tracings of the antennal afferents were obtained as described above. The lens of the lateral ocelli was removed in the same preparation. A dye droplet (either Dextran tetramethylrhodamine or Dextran, Alexa Fluor 488) was placed inside the ocellar retinae to be taken up by

TABLE 1 Antibody characterization

Antibody	Immunogen	Manufacturer; species; clonality; Cat #; RRID
Synapsin	*Drosophila* Synapsin glutathione-S-transferase fusion protein	E. Buchner, Theodor-Boveri-Institute, University of Würzburg, Germany; mouse; monoclonal; Cat # 3C11 (SYNORF1); RRID: AB_528479

second order afferent neurons. For double staining, combination of Dextran tetramethylrhodamine and Dextran, Alexa Fluor 488 was used. The dyes were incubated for 3–4 h in a dark humid chamber. The subsequent protocol was performed as described above for the pedicel staining.

Finally, all brains were scanned using a confocal laser-scanning microscope (Leica TCS SP8, Leica Microsystems GmbH, Wetzlar, Germany) with a 20x water immersion objective (20.0 × 0.7/0.75 NA) obtaining optical sections of 3 or 4 μm thickness. Image stacks were processed using ImageJ 1.52n (Wayne Rasband, National Institutes of Health, USA). To analyze the 3D structure of the JO projections, 3D renders of the tracings were created using the Amira "Voltex" module.

2.4 | Antibody characterization

To locate the central projections of JO and ocellar afferents in neuropils of the *Cataglyphis* brain, a monoclonal antibody to synapsin (SYNORF1, mouse@synapsin; kindly provided by E. Buchner and C. Wegener, University of Würzburg, Germany) was used for visualization of synapse-rich neuropils (Table 1). Synapsin is present in presynaptic terminals and highly conserved among invertebrates. The specificity of the antibody has been characterized previously for *Cataglyphis* ants (Schmitt, Stieb, Wehner, & Rössler, 2016; Schmitt, Vanselow, Schlosser, Wegener, & Rössler, 2017; Stieb, Hellwig, Wehner, & Rössler, 2012; Stieb, Muenz, Wehner, & Rössler, 2010) and most recently for *C. nodus* (Habenstein et al., 2020).

2.5 | Nomenclature

In this study, we refer to Habenstein et al. (2020) (see also https://www.insectbraindb.org for 3D data of the *Cataglyphis* brain) and Ito et al. (2014) for the nomenclature of the neuropils in the ant brain. The nomenclature of the JO and its sensory projections are in line with the nomenclature introduced for the honey bee (Ai et al., 2007).

3 | RESULTS

The antennae of *C. nodus* ants consist of three main segments: the scape is the basal segment located closest to the ant head, the second segment is the pedicel, which contains the JO, and the third is the flagellum, the most distal segment, comprising 10 flagellomeres (Figure 1a). The entire antenna is covered with evenly distributed small bristles. Only on the ventral side of the scape, the density of bristles is very scarce. A hair plate is located close to the joint of scape and pedicel (Figure 1b). At the joint of pedicel and flagellum, evenly distributed dents within the cuticle are located, indicating the location of attachment structures of the JO (Figure 1b).

3.1 | Organization of the JO

3.1.1 | Cross-sections of the pedicel

To get an insight into the anatomy of the JO and its sensory structures inside the antenna of *C. nodus*, the pedicel was sectioned in 1.5 μm thick cross-sections. In total, a pedicel of *C. nodus* produced about 556 cross-sections. The inside of the pedicel contains two antennal nerve branches (anterior (aAN) and posterior antennal nerve (pAN)), two tracheae (anterior (aTR) and posterior trachea (pTR)), and the antennal vessel (AV) that run through the entire antenna (Figure 2). At the distal most end of the pedicel, the JO is attached to the intersegmental membrane of the flagellum-pedicel joint via attachment cells (AC, sometimes called cap cells). These ACs are radially arranged along the cuticle walls of pedicel and flagellum (Figure 2b). The ACs comprise chitin caps (CAP) (Figure 2c). To each cap, one sensory unit of the JO, a so-called scolopidium, is attached (Figure 2d). In each adult worker of *C. nodus*, we investigated (n = 4) 40 scolopidia were found. The dendrites of the scolopidia proceed to the cell bodies that attach to the hypodermis of the pedicel in a ring-like manner (Figure 2f-g). In the middle of the pedicel, the axons of the scolopidia converge into three main JO nerves (JON1, JON2, JON3) (Figures 2h-j). At the proximal end of the pedicel, that is, close to the pedicel-scape joint, innervated hairs forming a hair plate (HP, sometimes called Böhm's organ or Böhm's bristles [Böhm, 1911]) are located (Figures 2j-k). Besides the HP bristles, only very rarely innervated bristles were found along the pedicel of *C. nodus*.

3.1.2 | Longitudinal sections of the pedicel

To get a more detailed understanding of the scolopidial structure of the JO in *C. nodus*, the pedicel was sectioned into 1.4 μm thick longitudinal sections. Scolopidia are elongated sensory structures arranged in a circle around the pedicel (see above). A scolopidium consists of an AC with a CAP embedded in the intersegmental membrane (Figures 3a-b). Attached to the caps are chitinous scolopale rods of scolopale cells (Figure 3c). The scolopale cells and rods ensheath the neuronal dendrites of the sensory cells. Each scolopidium comprises three sensory neurons. The total number of sensory neurons of the JO, therefore, was estimated with ~120. The scolopale dendrites continue to the cell bodies of the three sensory neurons (Figure 3c). At the distal end of the pedicel, no innervated bristles were found (Figure 3).

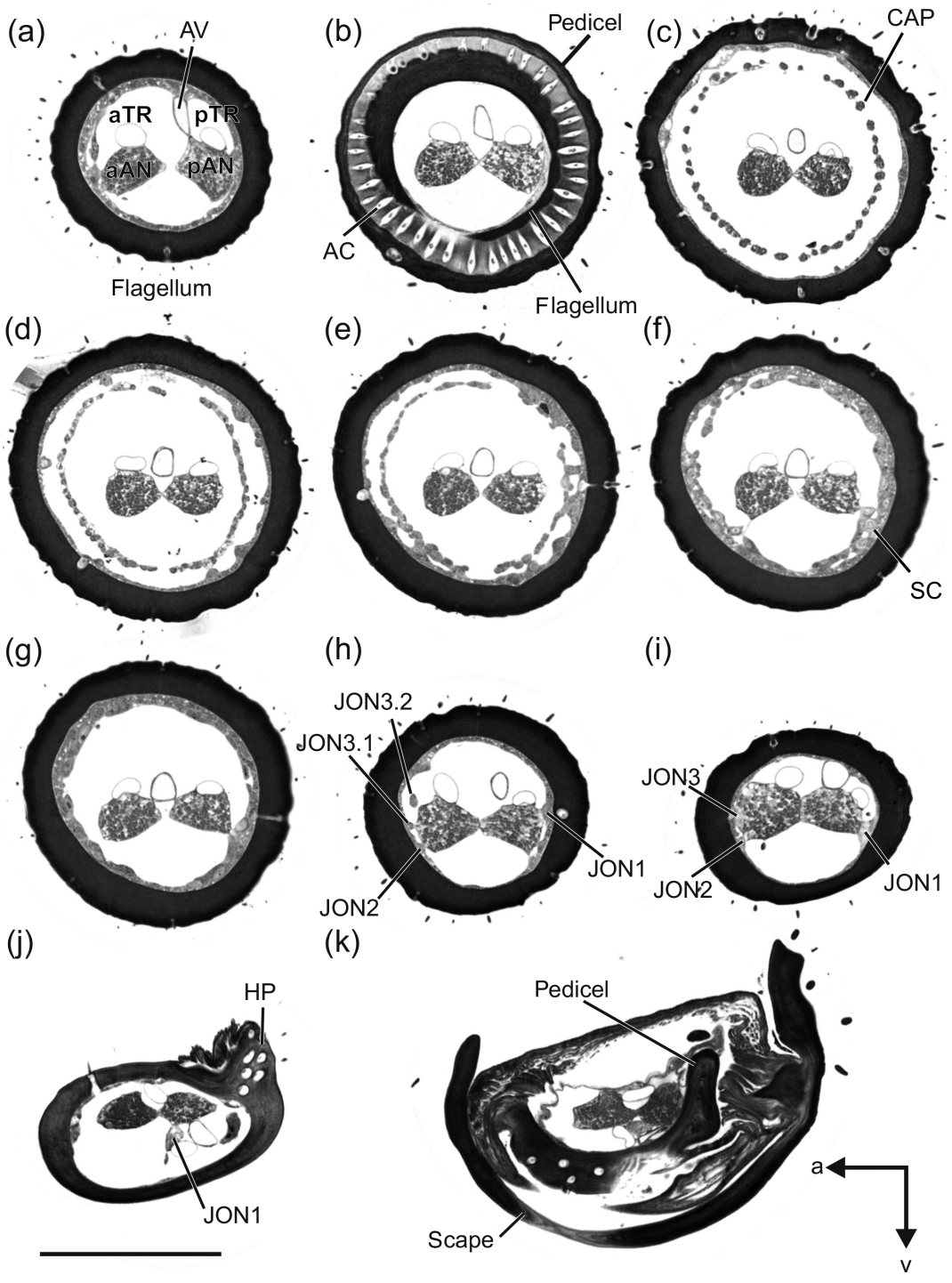

FIGURE 2 Serial cross-sections of the pedicel. The pedicel was sliced into 1.5 μm thick sections. Exemplary sections from the structures within the pedicel are shown. The position of the examples is depicted in the longitudinal views of 3D reconstructions in Figure 4 (bottom). The antennal vessel (AV), two antennal-nerve branches (AN, aAN, anterior antennal nerve; pAN, posterior antennal nerve), and two tracheae (TR, aTR, anterior trachea; pTR, posterior trachea) run along the entire pedicel. (a and b) Starting most distally—in the flagellum—the scolopidia of the Johnston's organ are attached to the intersegmental membrane via attachment cells (AC). (c) Chitin caps (CAP) are located at the most distal end of the scolopidia. (d and e) The elongated mechanosensory units of the JO (scolopidia) are distributed radially within the pedicel. (f and g) The neuronal cell bodies (SC) of the scolopidia are attached to the hypodermis in a circular fashion. (h–j) From there, the afferents of the JO converge into three nerve bundles (JON1-3). (j and k) Close to the joint between pedicel and scape, the hair plate (HP) sensilla are located on the dorsal side of the pedicel. Additional abbreviations: a, anterior; v, ventral. Scale bar 100 μm

3.1.3 | 3D reconstruction of the JO

The axons from sensory neurons within the 40 scolopidia converge in the middle of the pedicel into three JO nerves (JON1, JON2, JON3) (Figures 4 and 5). Each of these three JO nerves innervates a subsection of the JO scolopidia (Figure 4). JON1 innervates 20 posterior scolopidia of the JO and projects along with the pAN (Figures 4 and 5b). The other two nerves run along with and join the aAN. JON2 innervates four ventral JO scolopidia and JON3 16 anterior scolopidia (Figures 4 and 5c-d). The JO nerves project along the two AN branches before joining them close to the joint between pedicel and scape (Figure 5).

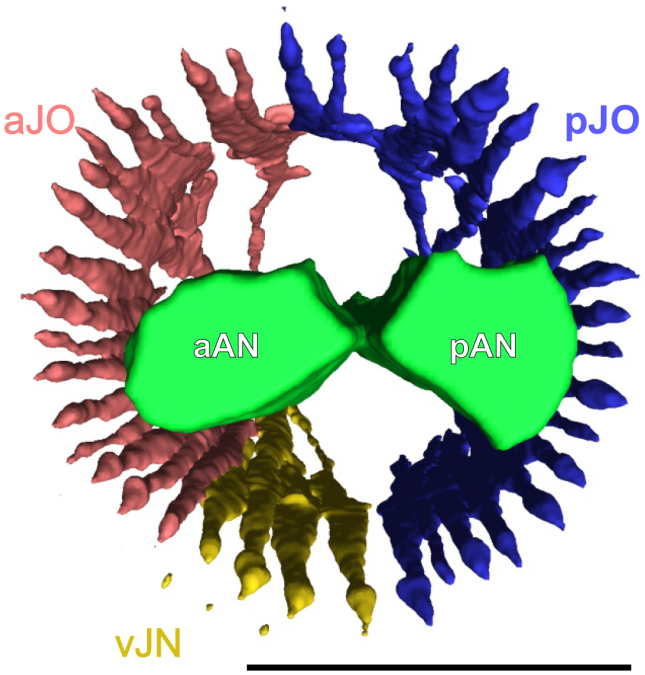

FIGURE 4 3D-reconstruction of the Johnston's organ (view from a distal perspective). The 40 scolopidia of the Johnston's organ (JO) in a *C. nodus* worker antenna (n = 4) are radially arranged around the antennal-nerve branches (AN, aAN, anterior antennal nerve; pAN, posterior antennal nerve). The JO scolopidia can be classified into three groups based on their afferent projections (see also Figure 5): The anterior JO (aJO, red) with 16 scolopidia, the posterior JO (pJO, blue) with 20 scolopidia, and the ventral JO (vJO, yellow) with 4 scolopidia. Scale bar 100 μm

3.2 | Central projections of the JO

In *Cataglyphis*, six bundles of axons from the sensory neurons of the antenna project into the brain. Four of these form distinct olfactory sensory tracts (T1-T4) that project into specific subsets of olfactory glomeruli in the antennal lobe (AL) (Stieb, Kelber, Wehner, & Rössler, 2011). Hence, the remaining two sensory tracts containing sensory afferents from the JO will be termed T5 and T6, respectively. This is in line with the antennal sensory tract nomenclature in the honeybee brain (Ai et al., 2007; Maronde, 1991). We used the recently published 3D atlas of the *C. nodus* brain to assign the antennal projections to distinct neuropils in the central brain (Habenstein et al., 2020; for 3D data, see https://www.insectbraindb.org).

As mentioned above, the afferents of the JO project along the two AN branches into the brain. As a first step, we analyzed anterograde tracings of antennal sensory projections that had been mass

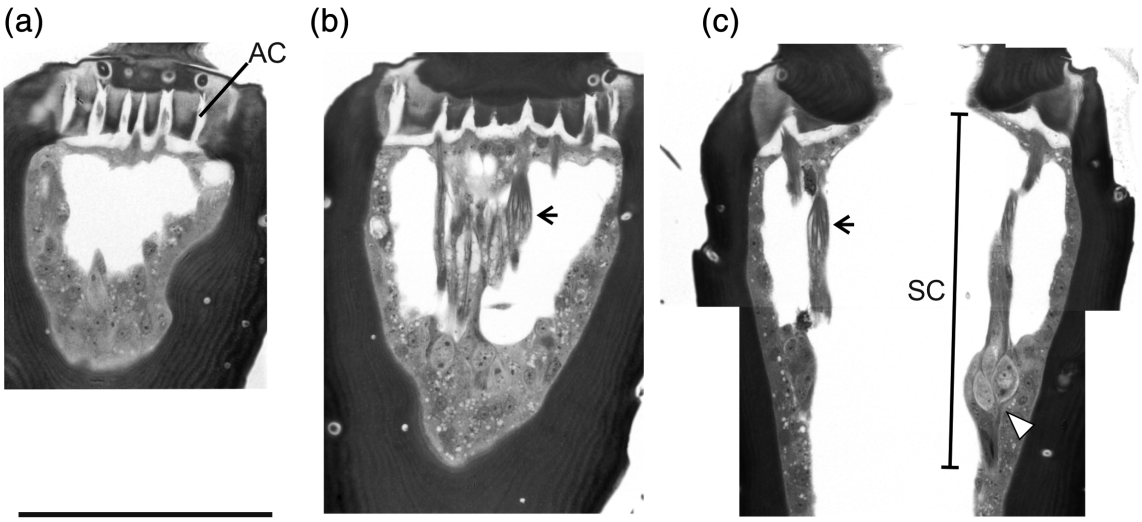

FIGURE 3 Serial longitudinal sections of the pedicel. The pedicel was sliced into 1.4 μm thick sections. (a) The scolopidia of the Johnston's organ are attached to the intersegmental membrane between flagellum and pedicel via attachment cells (AC). (b and c) The scolopidia are elongated mechanosensory structures. Each scolopidium comprises three dendrites from three sensory neurons. Scolopale rods (arrows) surround and enclose the dendrites. Three cell bodies (white arrowhead) of the sensory neurons (scolopale cells (SC)) of an individual scolopidium are attached to the hypodermis. Scale bar 100 μm

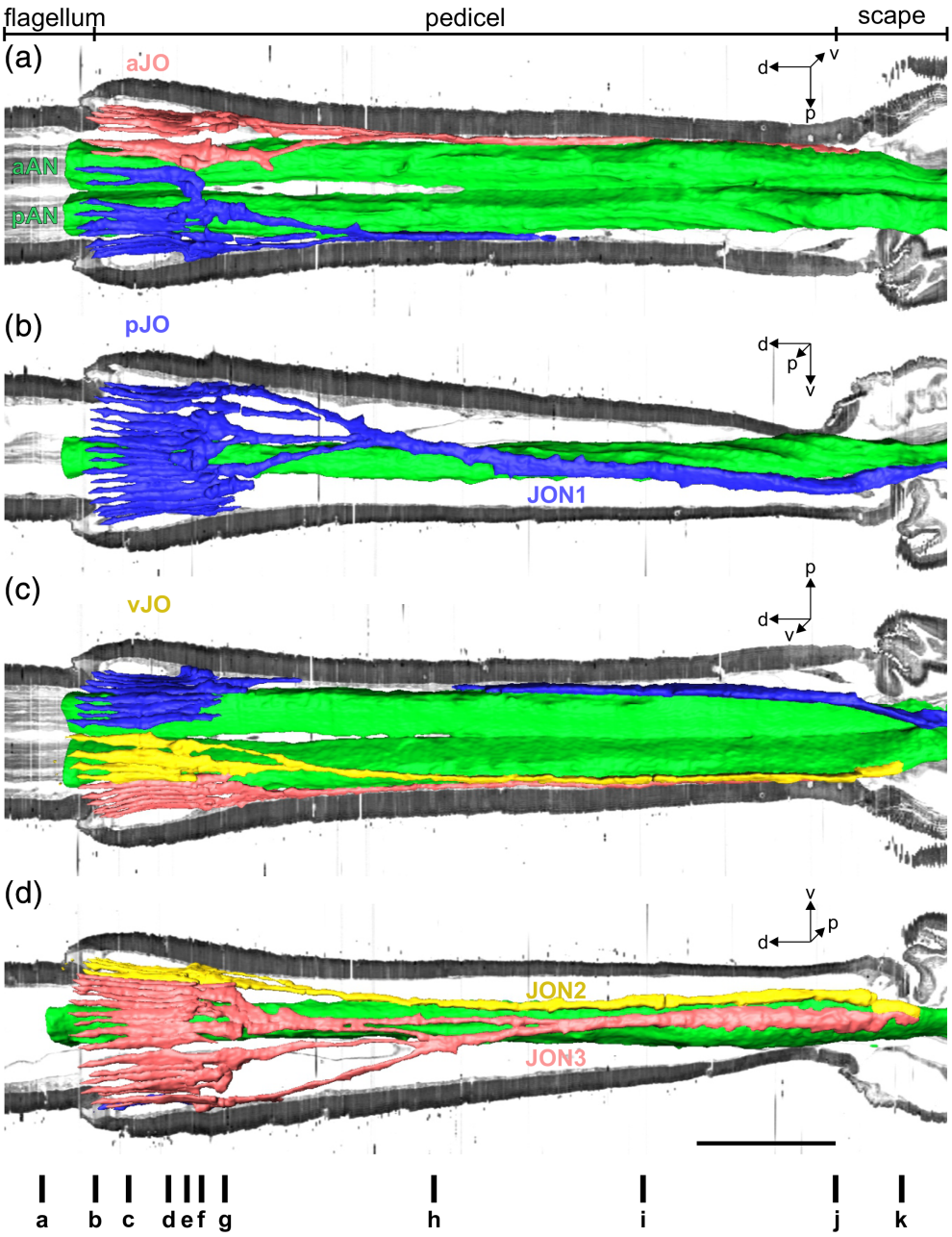

FIGURE 5 3D-reconstruction of the Johnston's organ (longitudinal perspectives). (a) View from dorsal, (b) posterior, (c) ventral, (d) and anterior. The scolopidia of the Johnston's organ (JO) are located in the distal third of the pedicel. Their neuronal afferents converge into three distinct axon bundles. Each axon bundle projects from a specific subset of scolopidia (compare Figure 4). Afferents of the posterior JO (pJO) join into JO nerve 1 (JON1, blue) and run along the posterior antennal-nerve branch (pAN). JO nerve 2 (JON2) contains the afferents of the ventral JO (vJO, yellow) and anterior JO (aJO) afferents join JO nerve 3 (JON3, red). Both JON2 and JON3 run along the anterior antennal-nerve branch (aAN). The positions of the exemplary cross sections shown in Figure 2 are indicated at the bottom (d). Additional abbreviations: d, distal; p, posterior; v, ventral. Scale bar 100 μm

filled by applying fluorescent dye at the level of the pedicel (n = 24). Antennal afferents from the flagellum and pedicel project into several distinct neuropils besides the AL (Figures 6a–e and 7). The respective central neuropils were identified by aligning the anti-synapsin stained neuropils with those described in the *Cataglyphis* brain atlas (Habenstein et al., 2020) (Figure 6f). The majority of antennal mechanosensory afferents projects to the AMMC (Figure 6a). A subset of the projections continues into the saddle (SAD) (Figure 6b-d), and, from there, a proportion of afferents projects into the ventral complex (VX) and the ventrolateral protocerebrum (VLP) (Figure 6b). At the most posterior end, a subset of mechanosensory afferents proceeds further into the posterior slope (PS) (Figure 6d). Another small group of projections goes further down into the gnathal ganglia (GNG) (Figure 6e). 3D reconstructions of the antennal afferents revealed an overview of the two mechanosensory tracts (T5, T6) and their terminal branching fields within distinct brain regions and with respect to other major brain neuropils (Figure 7). The afferents of T5 and 6 bypass the AL to most strongly innervate the AMMC and SAD. From there, a subpopulation of the axons proceeds and terminates in the VX, VLP, and the PS (Figures 6 and 7).

To differentiate the sensory axons associated with receptor neurons of the JO, a double anterograde staining procedure of the AN at the level of the first flagellomere and the pedicel was used (n = 10) (Figure 1c). This differential labeling technique revealed the projection patterns of antennal mechanosensory afferents derived from the JO (labeled in magenta only). The results show that JO afferents contribute to both mechanosensory tracts (T5 and T6, labeled in magenta or red) (Figure 8a). The projections from JO afferents split into two

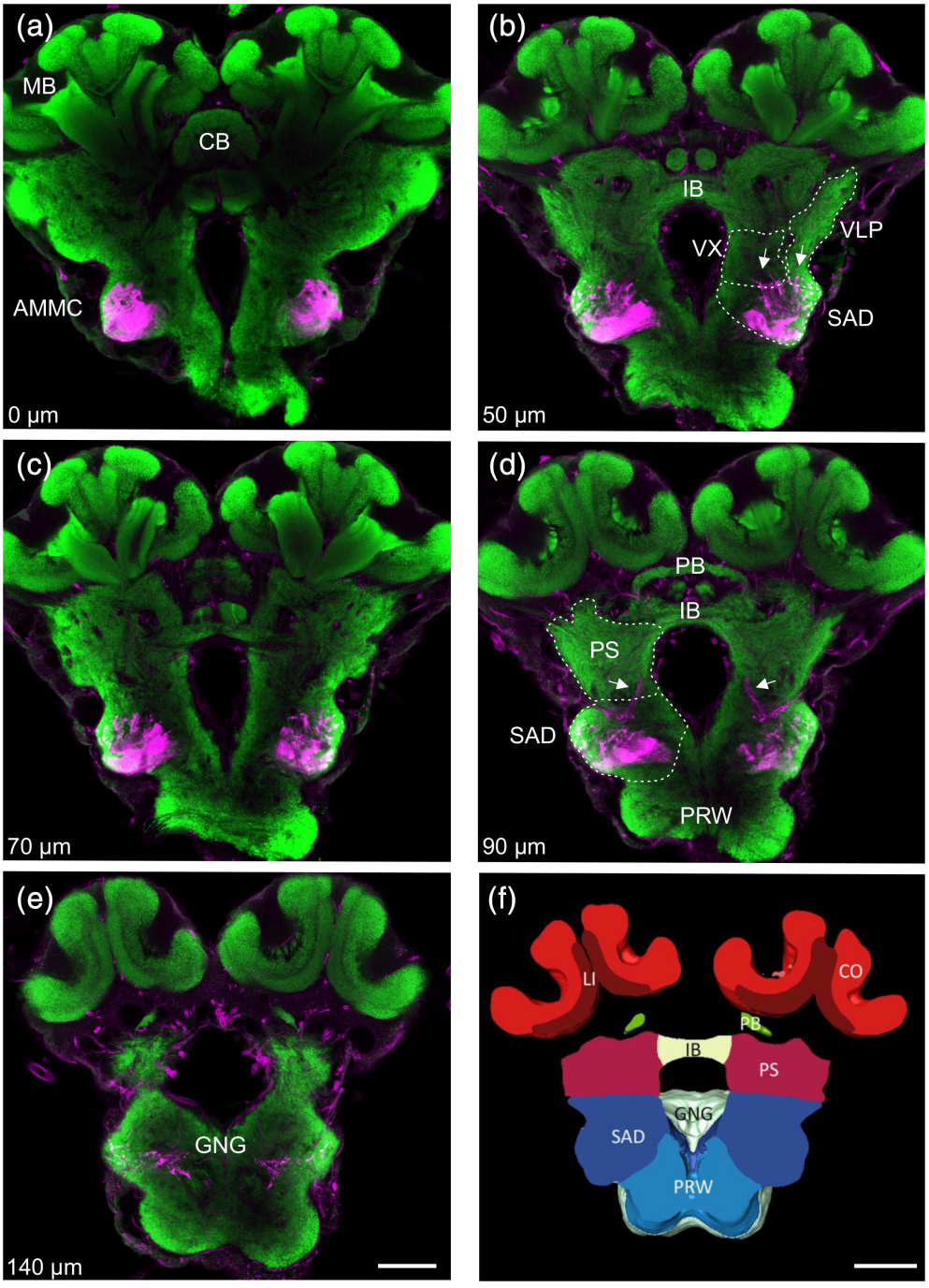

FIGURE 6 Overview of antennal mechanosensory afferent projections in the *C. nodus* brain. For the anterograde staining of antennal afferent projections (magenta), the antenna was cut at the level of the pedicel and a fluorescent dye was applied (see scheme in Figure 1c). The brain was subsequently treated with an anti-synapsin antibody to label synapse-rich neuropils (green). (a–d) The labeled projections (magenta) first converge in the antennal mechanosensory and motor center (AMMC) and, more posteriorly, proceed into the saddle (SAD). The 3D atlas from Habenstein et al. (2020) was used as a reference to identify the central neuropils. (b) Some of the afferents run further to terminate in the ventral complex (VX) and the ventrolateral protocerebrum (VLP). (d and e) At the most posterior end, antennal afferents terminate the posterior slope (PS), and some fibers proceed down into the gnathal ganglia (GNG). (f) Reconstruction of the *C. nodus* brain showing synapsin-rich neuropils and their boundaries at roughly the same depth as in (d) (image from Habenstein et al., 2020). Please note that the section in (d) is slightly tilted compared to the section from the *C. nodus* brain atlas (f), which was taken into account for the identification of synapsin-rich central neuropils. In the lower-left corner of each panel, the depth in relation to (a) is indicated. Each level shown comprises a projection of three optical sections (thickness 3 µm each). Confocal images obtained with 20x objective and 0.75 zoom. Additional abbreviations: CB, central body; CO, collar; IB, inferior bridge; LI, lip; MB, mushroom bodies; PB, protocerebral bridge; PRW, prow. Scale bars in (e) and (f) 100 µm

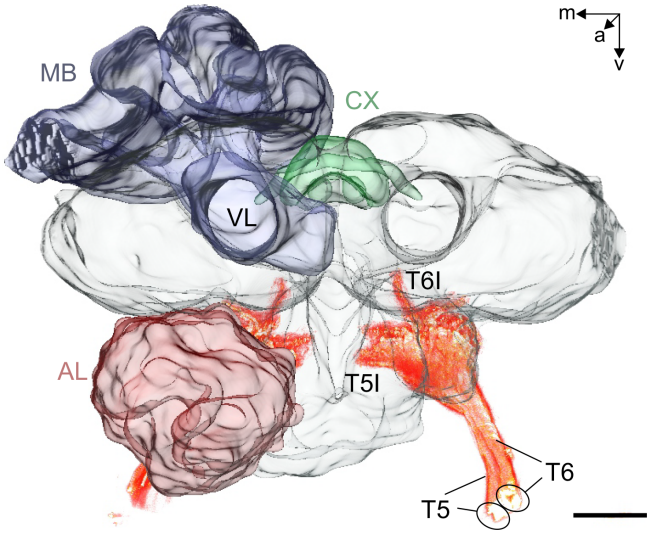

FIGURE 7 3D reconstruction of the projections of antennal mechanosensory afferents in the *C. nodus* brain. The antennal mechanosensory nerve bundles include two fiber bundles from the Johnston's organ (T5, T6). The projections bypass the antennal lobe (AL) and project into the AMMC. From there, a subset of afferents project further into the central brain. T6I projects most posteriorly, while T5I terminates more anteriorly (see more details in Figure 6). Additional abbreviations: a, anterior; CX, central complex; m, medial; MB, mushroom bodies; v, ventral; VL, vertical lobe, . Scale bar 100 μm

terminal branching fields, T5I and T5II at the level of the AMMC (Figure 8b-c). Branches in T5I are ventromedially to the ventral region of the AMMC with some fibers continuing to the SAD, and terminal branches in T5II are dorsolaterally to the dorsal region of the AMMC (Figure 8b). Further axons bypass the AMMC before branching into three collaterals (T6I-T6III). These very likely represent sensory axons exclusively from the JO. The axons forming T6I project most posteriorly and terminate in the PS, whereas T6II and III branches are located in the SAD, VX and VLP (Figure 8c, e-f).

We labeled sensory projections form ocellar neurons to compare their central projections with those from JO afferents. Projections from the lateral ocelli run through the PS and SAD and form branches in the PS, in exactly the same region as terminals from the JO (T6I) (n = 16) (Figure 9a). Analyzes of small substacks of optical sections revealed that T6I axons and axons from secondary interneurons of the ocelli are in very close apposition within the same region in the PS (n = 6) (Figure 9b). Some of the overlapping branches may proceed further into the SAD. Axons of T6II terminate in the VX, whereas T6III axons terminate in the VLP region (Figure 8b).

3.3 | Organization of the JO in virgin queens and males

As a first step to compare the JO of the flight enabled reproductive castes with the ambulatory worker caste of *C. nodus*, we produced exemplary serial cross-sections of the pedicel of virgin queens and males. To estimate potential differences of the antennal segments, scanning EM images were obtained. These show that the pedicel of worker ants is 157 μm in diameter and 627 μm in length (n = 1) (Figure 10a-c). In queens, the pedicel is 169 μm in diameter and 639 μm in length (n = 1) (Figure 10d-f). The pedicel of males is the largest with 195 μm in diameter and 652 μm in length (n = 1) (Figure 10g-i).

As in *C. nodus* workers, the JOs of the reproductive castes are arranged radially within the distal portion of the pedicel. Here, at the joint between pedicel and flagellum, the scolopidia of the JO are attached to the intersegmental membrane. In the example of a *C. nodus* male we found 48 (n = 1) scolopidia, while the virgin queen had 42 (n = 1) (Figure 10). Both, males and queens, have three sensory neurons associated with each scolopidium. Based on this, the number of sensory neurons in the JO can roughly be estimated with ∼144 in males and ∼ 126 in queens. In workers and queens, the diameter of the ANs is similar, while the ANs in males are strikingly thicker. Overall, the pedicel of males is more densely packed with cellular tissue than their female counterparts (Figure 10).

4 | DISCUSSION

This study, for the first time, analyzes in detail the three dimensional structure of the JO in the antenna of an ant of the genus *Cataglyphis* (desert ants) together with its afferent projections into the central brain of the ant. The JO scolopidia are attached to the intersegmental membrane between flagellum and pedicel via the chitinous caps of the attachment cells. Scolopale rods that are attached to the caps ensheath three neuronal dendrites in each scolopidium. In *Cataglyphis* workers, the 40 scolopidia are arranged radially within the pedicel. They can be classified into three groups based on their afferent innervations. JO sensory neurons project into the AMMC and the SAD via the T5 fiber bundle. The T6 projections from the JO bypass the AMMC, proceed via the SAD, and terminate in the VX, VLP, PS, and GNG. Projections from the ocelli have branches in close apposition with JO terminals within the PS. While the overall structure of the JO is similar between the different castes of *Cataglyphis*, the number of scolopidia differs mainly between males and the two female castes.

4.1 | Morphology of the JO

The JO of *C. nodus* is located at the distal end of the second antennal segment, the pedicel. It is attached to the intersegmental membrane at the joint of pedicel and flagellum. The attachment sites of its subunits can be seen on the pedicel cuticle as small pits. This general morphology of the sensory units in the JO of *C. nodus* resembles the JOs of most other insect species investigated (review: Yack, 2004). In *C. nodus*, each JO scolopidium contains three sensory neurons. This is in line with most other insects, with the exception of only a few Diptera with only two sensory neurons per scolopidium (Schmidt, 1974;

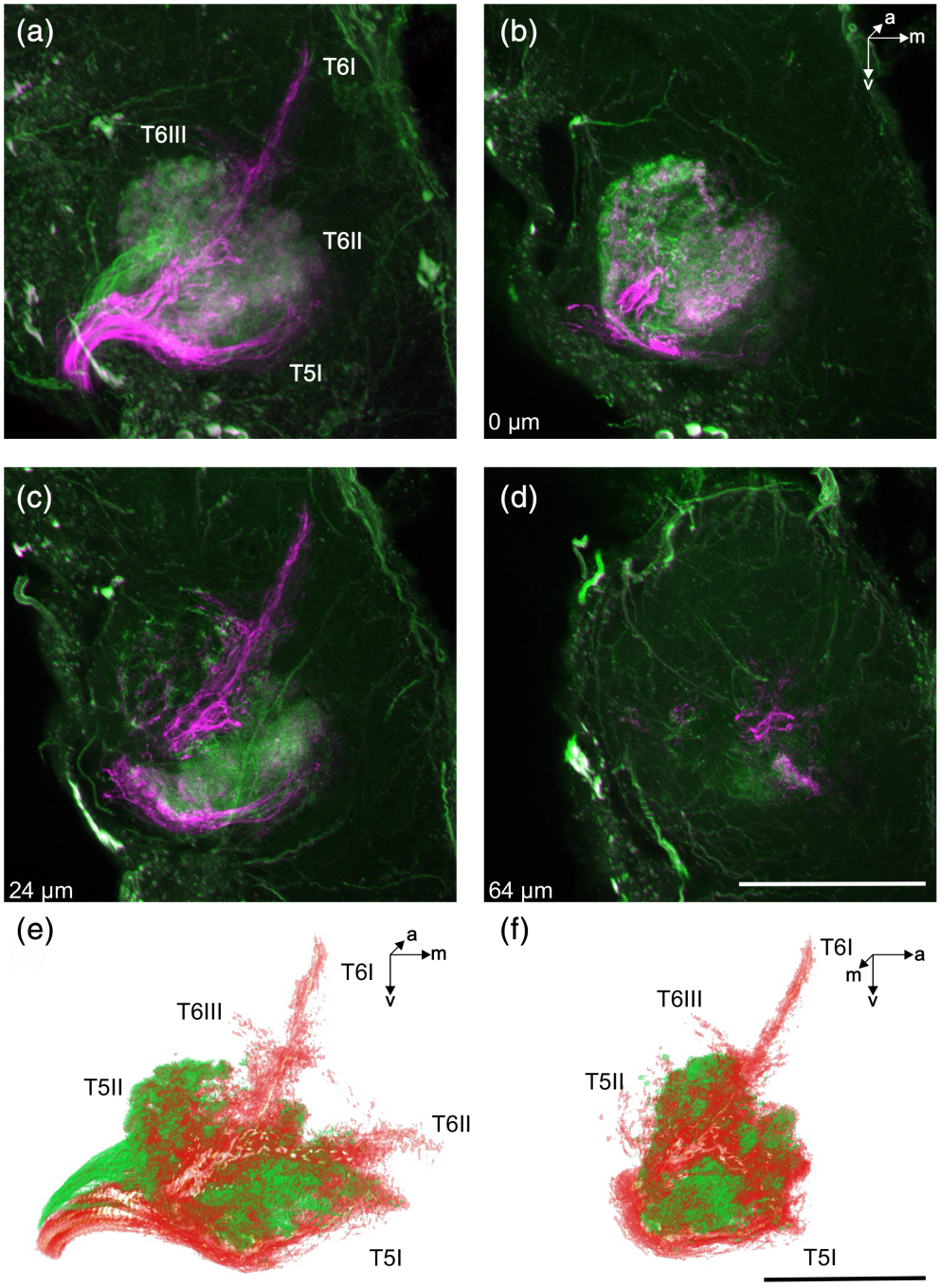

FIGURE 8 Differential tracing of Johnston's organ afferents and 3D-reconstruction. The Johnston's organ (JO) afferents were selectively stained using an anterograde double-tracing procedure (see methods and Figure 1c). Mechanosensory projections of the antenna are shown in green or merged green/magenta, while projections of the JO are labeled in magenta only. (a) Overview of the differentially labeled projections of the JO (magenta). While most other antennal mechanosensory projections terminate in the antennal mechanosensory and motor center (AMMC) (b) and saddle (SAD) (c), the two fiber bundles of the JO (within T5 and T6) proceed further into more posterior brain areas. T5 splits into two branches with T5I projecting to the ventral region of the AMMC (b) with some fibers continuing to the SAD (c), and T5II projects to the dorsal region of the AMMC (b). T6 bypasses the AMMC and splits into three branches. T6I terminates most posteriorly in the PS (c) (compare with Figure 6). T6II terminates in the ventral complex (VX) and T6III in the ventrolateral protocerebrum (VLP) (c). Some neurites project further ventrally into the gnathal ganglion (GNG) (d). (b–d) In the lower left corner of each panel, the depth relative to (b) is indicated. Each panel shows a projection of optical sections (thickness of 3 µm each) (a) comprises a projection of 83 optical sections, (b, c) comprise a projection of four optical sections, respectively; (d) comprises a projection of six optical sections). Confocal images using a 20x objective and 2.40 zoom. (e, f) Two views of 3D-reconstruction of the JO afferents (red) and other antennal mechanosensory projections (green). Scale bars in (d) and (f) 100 µm

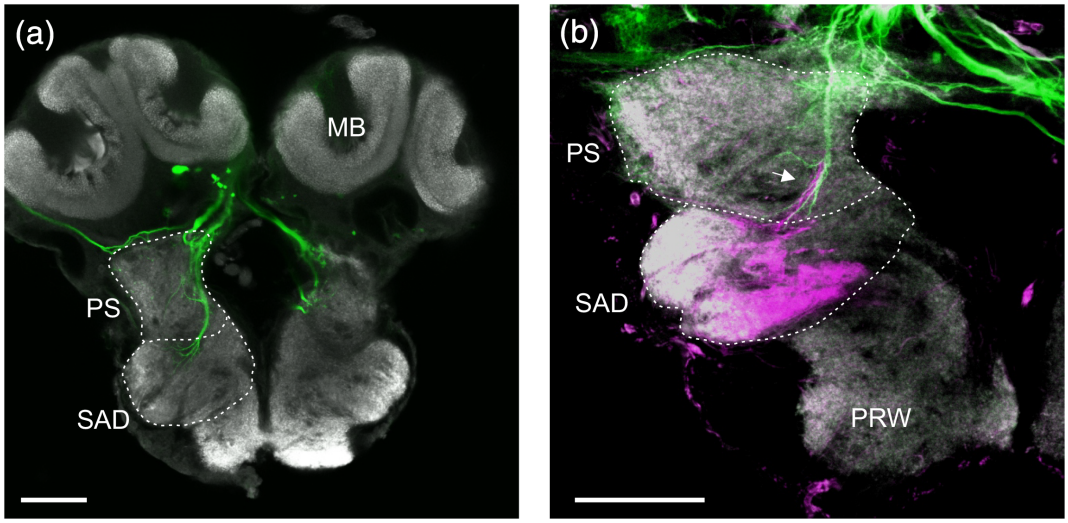

FIGURE 9 Differential tracing of afferents from the lateral ocelli and the Johnston's organ. (a) Afferent neurons from the lateral ocelli (green) project into the posterior slope (PS) and the saddle (SAD). (b) In the PS, projections from the ocelli (green) and Johnston's organ projections terminate in very close proximity to each other. Confocal images using a 20x objective and (a) a 0.75 zoom or (b) a 1.50 zoom. Each panel shows a projection of three optical sections (thickness of 3 μm each). Additional abbreviations: MB, mushroom bodies, PRW, prow. Scale bars in (a) and (b) 100 μm

Uga & Kuwabara, 1965). With a total number of 40 scolopidia, the number of scolopidia in the JO of adult *C. nodus* workers is rather low, compared to other insects. In general, the JO exhibits a wide range in scolopidial numbers and associated sensory neurons across the insects (Snodgrass, 1926). While the JO of *C. nodus* contains only 120 sensory neurons, the JO of mosquitos may hold up to 30,000 sensory neurons (Boo & Richards, 1975). Even when compared to smaller JOs, like the one in *D. melanogaster* with 720 sensory neurons, the numbers in the JO of *Cataglyphis* are still rather small. Interestingly, also other Hymenoptera were shown to possess JOs comprising small cell numbers (Snodgrass, 1926; Vowles, 1954). Honeybees are in a comparable range like *D. melanogaster* with about 720 neuronal cells in 240 scolopidia (Ai et al., 2007), and the JO of sawflies consists of about 750 neuronal cells in 250 scolopidia (Hallberg, 1981). In contrast to ant workers, however, mosquitos, fruit flies, bees, and sawflies are capable of flight. The JO is an important organ for flight control and helps flying insects to keep their posture during flight (Sane et al., 2007). Surprisingly, however, the sexual castes of *C. nodus* that are capable of flight (male and queen), only show a slightly higher number of scolopidia and associated sensory neurons in the JO. Therefore, a stronger effect on the number of scolopidia in the JO may be ascribed to the capability of hearing. While mosquitos (Cator et al., 2009; Göpfert & Robert, 2001a), fruit flies (Göpfert & Robert, 2001b; Göpfert & Robert, 2002), and honeybees (Dreller & Kirchner, 1993a; Dreller & Kirchner, 1993b; Dreller & Kirchner, 1995) detect airborne sound using the JO, ants are deaf (Roces & Tautz, 2001) suggesting that the JO of ants does not serve as a sensory organ for the detection of airborne sound. Compared with other ant species investigated so far, the dimensions of the JO in *Cataglyphis* are much more similar. *Formica* wood ants have a JO comprising only 20 scolopidia (about 60 sensory neurons) (Vowles, 1954), and *Camponotus* (carpenter) ants possess about 55 scolopidia with 165 estimated sensory neurons (Masson & Gabouriaut, 1973).

Similar to all species studied so far, the scolopidia in *C. nodus* are attached to the intersegmental membrane by chitin caps, which are connected to scolopale rods. Antennal deflection is transferred via these structures and, as a result lead to the opening of mechanosensitive ion channels in the sensory dendrites upon stimulation. The resulting action potentials are relayed to the central brain (Todi et al., 2004). In *C. nodus*, the afferent projections of sensory neurons within scolopidia of the JO are bundled into three distinct nerves. Similar to the situation in *A. mellifera* (Ai et al., 2007), these three JO nerves are supplied by specific subsets of scolopidia, respectively. The posterior scolopidia of the JO in bees (Ai et al., 2007) and *C. nodus* (approx. half of the total number of scolopidia) join JON1, the anterior scolopidia converge into JON2, and ventral scolopidia into JON3. However, whereas the scolopidial subgroups are clustered within the pedicel of *A. mellifera* (Ai et al., 2007), in *Cataglyphis* they are very neatly aligned along an evenly spaced circle within the pedicel. This radial arrangement of the scolopidia can also be found in other insects, including other ant species (Masson & Gabouriaut, 1973; Vowles, 1954), fruit flies (Schmidt, 1974), and sawflies (Hallberg, 1981).

4.2 | Neuronal projections of the JO

The overall neuronal projection patterns of the JO afferents in *C. nodus* show a high degree of similarity with those described in the honeybee (Ai et al., 2007; Brockmann & Robinson, 2007) and *Drosophila* (Kamikouchi et al., 2006). The most prominent part of the JO afferents projects to the AMMC (T5 tract). There the JO afferents

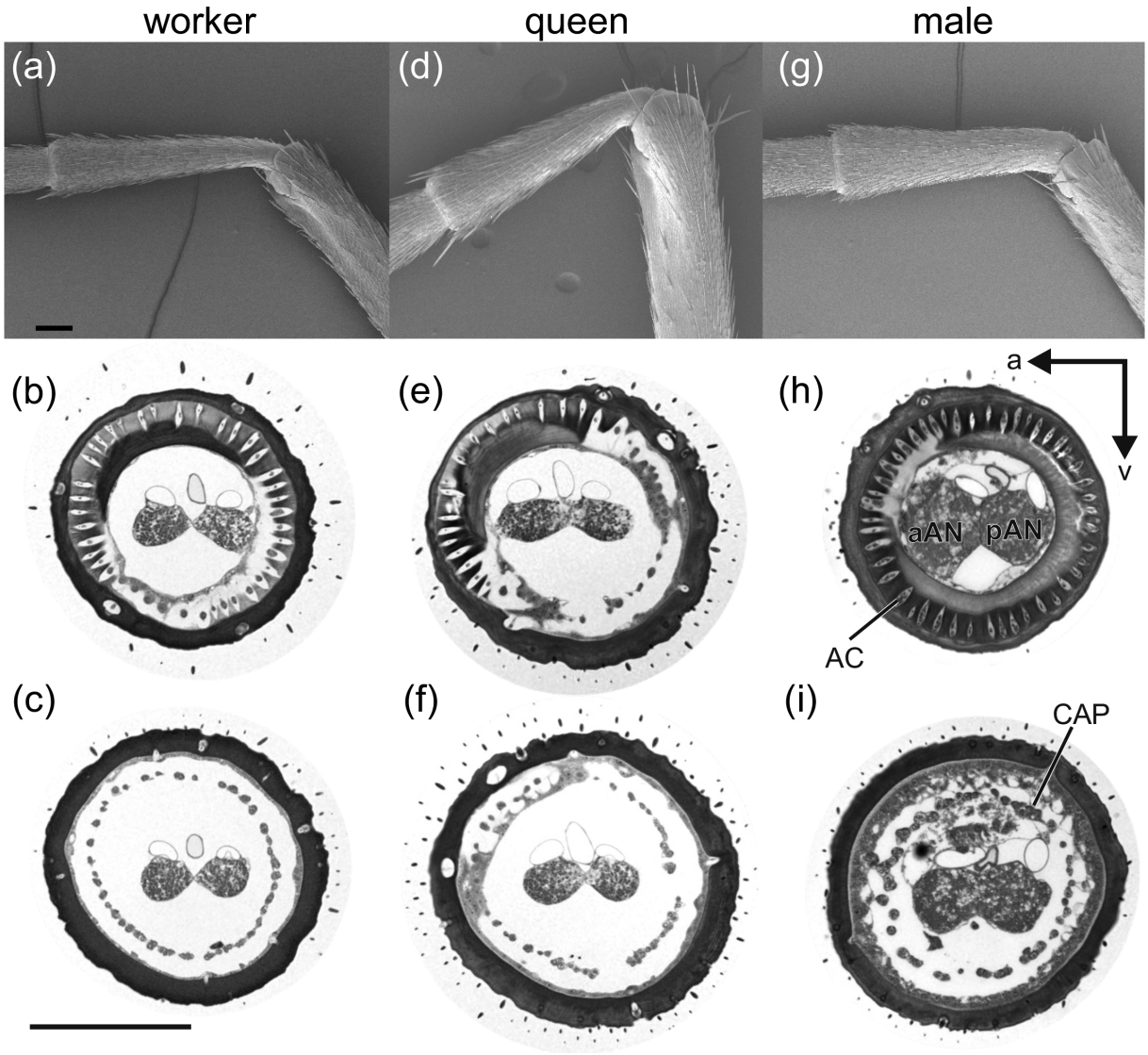

FIGURE 10 Comparison of the pedicel and the Johnston's organ between a *C. nodus* worker, queen and male. Polymorphism between the two female castes and males in *C. nodus*. (a–c) Worker, (d–f) queen, and (g–i) male. (a, d, g) Scanning electron microscopy images of the pedicel in the two females castes and males. The pedicel of workers (a) is smaller compared to the situation in queens (d). The longest and widest pedicel was found in males (g). (b, c, e, f, h, i) Exemplary cross-sections at different levels of the pedicel (1.5 μm thickness). While the overall structure of the Johnston's organ (JO) is similar in the female castes and males, the number of scolopidia differs slightly. (b and c) The JO in the worker antenna comprises 40 scolopidia (n = 4), (e and f) the JO of a queen comprises 42 scolopidia (n = 1), and (h and i) the JO of a male comprises 48 scolopidia in the JO (n = 1). For details see text. Abbreviations: aAN, anterior antennal nerve; AC, attachment cells; CAP, scolopale cap; pAN, posterior antennal nerve. (a–c) For better comparison, the exemplary images of the worker antenna were taken from Figures 1 and 2. Scale bars in (a) and (c) 100 μm

form a somatotopic map in *Drosophila* (Kamikouchi et al., 2006), honey bees (Ai et al., 2007), and mosquitos (Ignell, Dekker, Ghaninia, & Hansson, 2005). In *Drosophila*, antennal deflection by wind is represented in a map-like manner in the AMMC (Yorozu et al., 2009). Wind compass information is then transferred to the central complex (CX) (Okubo et al., 2020). In the CX, wind information is integrated into the path integrator of the insect brain (Honkanen, Adden, Freitas, & Heinze, 2019), where it is combined with visual cues to allow for multimodal spatial orientation (Okubo et al., 2020).

The T6 nerve tract of the JO afferents bypasses the AMMC and projects into more posterior neuropils. In *C. nodus*, JO afferents terminate in the VX (T6II) and the VLP (T6III). These projections show similarities with those in *Drosophila* (Kamikouchi et al., 2006) and the honeybee (Ai et al., 2007). Selective staining of individual JO nerves in the honeybee revealed that subgroups of JO scolopidia (pJO, aJO, vJO) have similar overall projection patterns, and only terminal branches of vJO in T6I were segregated from those of aJO and pJO (Ai et al., 2007). Whether this is also the case in *Cataglyphis* could not be resolved with our double staining technique. The pedicel of *Cataglyphis'* antennae is very thin and surrounded by thick cuticle, which renders access to individual JO nerves or sensory neurons impossible. It therefore remains unclear whether the three groups of

JO receptor neurons represent functional groups or, alternatively, the projections via three nerves may reflect a developmental pattern. Ideally, future studies might be able to combine functional analyzes with projections of individual JO receptor neurons using intracellular recording and staining from a more proximal position of the nerves to resolve this.

In *Cataglyphis*, both the VX and VLP receive visual input from the primary optic ganglia (medulla, lobula) via the posterior (POC) and inferior (IOC) optic commissures (Habenstein et al., 2020). In the honeybee, similar visual projections into this area were found (Maronde, 1991). Interestingly, in the PS terminals of the T6I tract from the JO converge with terminals of sensory neurons from the ocelli. A similar finding has been reported in the honeybee (Ai et al., 2007; Pareto, 1972). In *Cataglyphis*, the ocelli were shown to be polarization sensitive (Fent & Wehner, 1985; Mote & Wehner, 1980) and the photoreceptor neurons contain untwisted rhabdomeres (Penmetcha, Ogawa, Ribi, & Narendra, 2019). This indicates that multimodal navigational cues from the ocelli and the JO converge in this brain region. Whether the two sets of neurons directly synapse on each other or, more likely, converge on multimodal interneurons still needs to be shown using EM techniques. Due to their multisensory input from different primary (visual and mechanosensory) channels, the PS was recently defined as another multisensory integration center in the *Drosophila* brain (Currier & Nagel, 2020). Our results indicate that in addition to the PS, the VX and VLP may also serve as multimodal integration regions.

4.3 | JO as a multisensory organ in *Cataglyphis*

4.3.1 | Flight control or sexual dimorphism?

Since the JO of ants contains a rather small number of scolopidial units and is not involved in hearing, it is a perfect candidate to study its potential involvement in other sensory modalities. Additionally, ants provide the unique feature to compare the JO in ambulatory and flying individuals within the same species. The reproductive castes of *Cataglyphis* ants are winged and capable of flight, while the worker caste is purely ambulatory (Peeters & Aron, 2017). Interestingly, our first results show that the difference in the number of JO scolopidia between ambulatory and flying *C. nodus* is only marginal. Workers have the lowest (and very invariant) number of scolopidia, followed by an only marginally higher number in a queen, but a clearly higher number in a male. This result corresponds with findings in honeybees (McIndoo, 1922). *A. mellifera* workers have, as in *C. nodus*, the lowest number of scolopidia with about 70 scolopidia (in *C. nodus* 40 scolopidia). This is closely followed by honeybee queens with 72 (in *C. nodus* 42) and with some distance the drones (males) with 100 caps in the intersegmental membrane (in *C. nodus* 48 scolopidia) (McIndoo, 1922). Importantly, in the honeybee, both female castes and males are capable of flight. However, in both the honeybee and in *C. nodus*, only the number of scolopidia in males is substantially higher compared to the situation in both female castes. This suggests that in both cases, the honeybee and the ant, the differences in scolopidia numbers are not linked to the capability of flight. However, the JO could still play a role during *Cataglyphis'* courtship, which requires further investigation.

4.3.2 | JO as a wind compass

Elaborated navigational skills play a crucial role in the survival of foraging ants. In addition to their largely visually guided path integrator, *Cataglyphis* ants also employ orientation strategies based on information about wind direction. This allows the ants to find the scattered food items in their meager environment, to pinpoint their nest entrance (Steck et al., 2009; Wolf & Wehner, 2000), and to navigate at night (Wehner & Duelli, 1971). The ants are even able to track their displacement by wind and correct for it (Wystrach & Schwarz, 2013). Especially in their desert and desert-like habitats, these displacements can be quite significant. Desert ants constantly track wind directions in order to account for dislocations (Wystrach & Schwarz, 2013). Previously, it was shown by manipulation experiments that the antennae and especially the ability to move the joints of the antennal segments are essential for anemotactic orientation in desert ants (Wehner & Duelli, 1971; Wolf & Wehner, 2000). This makes the JO the most likely candidate for a wind compass in *Cataglyphis* ants.

The JO was also shown to detect multiple modalities and can be viewed as a multisensory organ. In *D. melanogaster*, the JO is able to distinguish between sound and wind information (Yorozu et al., 2009). The different stimuli activate different subsets of sensory neurons within the JO. Sound-sensitive neurons in the JO are phasically activated, while wind-sensitive neurons are tonically activated (Yorozu et al., 2009). Interestingly, each scolopidium in *D. melanogaster* houses one sound- and one wind-sensitive neuron (Ishikawa, Fujiwara, Wong, Ura, & Kamikouchi, 2020). The different sensory neurons also project to distinct parts of the AMMC, and wind direction is even represented in a map-like manner (Yorozu et al., 2009). These properties allow the JO to function as a multisensory organ. Wind compass information in *Drosophila* is conveyed from the terminal regions of the T6 tract into the CX (Okubo et al., 2020), a center for path integration in the insect brain (Honkanen et al., 2019). Interestingly, our results show that JO afferents in *Cataglyphis* contribute to two distinct projection regions within the AMMC. Future studies will be necessary to determine, if the JO afferents in *C. nodus* terminate in a map-like manner in the AMMC as they do in *Drosophila* (e.g. Yorozu et al., 2009).

4.3.3 | JO as gravity detector

While *D. melanogaster* is typically described as having two sensory neurons in each scolopidium of the JO (Uga & Kuwabara, 1965), more recent studies have shown that a significant subset of scolopidia comprise three neuronal cells (Todi et al., 2004). Todi et al. (2004) proposed that these additional sensory neurons could be used for sensing the gravitational force. Also in ants, the JO has been proposed

to be involved in graviception (Beckingham, Texada, Baker, Munjaal, & Armstrong, 2005; Vowles, 1954). For desert ants, the reception of the gravitational force plays an important role during path integration. *Cataglyphis* measures the walked distance during foraging trips via a step integrator (Wittlinger, Wehner, & Wolf, 2006). However, to estimate the correct distance from the nest, *Cataglyphis* has to take the slopes on its way into account and integrate this information into its path integrator (Grah & Ronacher, 2008; Grah, Wehner, & Ronacher, 2005; Ronacher, 2020). In contrast to other ants (Markl, 1962; Markl, 1963), bristle fields on the ants' body do not seem to be involved in the reception of gravitational forces in *Cataglyphis* (Wittlinger, Wolf, & Wehner, 2007). Up to now, the mechanism by which *Cataglyphis* measures slopes still remains elusive (Ronacher, 2020). The JO is a promising candidate to fulfill this function in gravity reception. In fact, in *D. melanogaster* the primary sensory organ for detecting gravity seems to be the JO (Kamikouchi et al., 2009). The ring-like arrangement of the scolopidia in the JO in *Cataglyphis* might even promote this function. Due to the different location of the scolopidia, some of the sensory neurons would always be maximally stretched, independent of antennal movement (Kamikouchi et al., 2006). This would allow the JO to distinguish between several tonic sensory inputs. It is likely, however, that other mechanosensory receptors, especially on the legs, like hair plates at the leg joints, or stretch receptors inside the leg, could be involved in gravity perception. Future studies are needed to investigate the involvement of the JO and other mechanoreceptors in the slope estimation in *Cataglyphis* ants.

4.3.4 | Potential multimodal contributions of the JO to navigation in *Cataglyphis*

The JO is a highly multimodal sensory organ involved in flight control and the reception of sound, wind, and gravitation. Its afferent projections in *Cataglyphis* extend beyond the AMMC into other parts of the central brain including the SAD, VX, VLP and PS. Interestingly, the PS was recently considered as a multimodal integration center in *Drosophila* (Currier & Nagel, 2020). It receives input from the ocelli in *Cataglyphis* and also in the honeybee (Ai et al., 2007; Pareto, 1972). Since the ocelli in *Cataglyphis* are sensitive to polarized light (Penmetcha et al., 2019), the convergences of information from the JO (possibly a wind compass and a graviceptor) with information from the sun compass would allow the PS to be a suitable candidate neuropil to synchronize or even calibrate these two compass systems. Additionally, the terminal areas of T6 afferents in the VX and VLP may also converge with information from afferent projections from the optic lobes (Habenstein et al., 2020; Ibbotson & Goodman, 1990; Maronde, 1991). This might allow for processing both input from the visual surrounding (panorama) and directional (polarized) skylight cues with information from the JO. The combination of visual information, sky compass information, as well as wind compass information from the JO, might allow naïve *Cataglyphis* ants to calibrate their visual navigational systems with geostable directional reference systems such as gravitational forces. This calibration is crucial for naïve ants to become successful navigators (Fleischmann, Christian, Müller, Rössler, & Wehner, 2016; Fleischmann, Grob, Wehner, & Rössler, 2017; Fleischmann, Rössler, & Wehner, 2018; Wehner, Meier, & Zollikofer, 2004). During the first excursions outside of the nest, the ants have to calibrate their compass systems and learn their surroundings (Grob, Fleischmann, & Rössler, 2019). These learning walks also correlate with structural synaptic plasticity along two visual pathways (Grob, Fleischmann, Grübel, Wehner, & Rössler, 2017; Rössler, 2019). Interestingly, in contrast to experienced foragers, *C. nodus* does not use celestial compass cues during first learning walks outside the nest entrance (Grob et al., 2017)—at the transition from inside the dark nest to outdoor foraging. During this phase the ants rather rely on the earth's magnetic field as their sole compass cue (Fleischmann, Grob, et al., 2018). This suggests that the ants use the earth's magnetic field as an earthbound reference to calibrate their internal celestial compass (review: Grob et al., 2019). The multimodal nature of the JO makes it a suitable candidate to play a crucial role during learning walks. In addition, the insect antennae have been suggested as a potential site for magnetoreception (de Oliveira et al., 2010; Guerra, Gegear, & Reppert, 2014; Lucano, Cernicchiaro, Wajnberg, & Esquivel, 2006), which renders the antenna and potentially the JO as one candidate in the search for the insect magnetic compass (Fleischmann, Grob, & Rössler, 2020).

Future combinations of behavioral manipulations with physiological and anatomical studies in *Cataglyphis* ants are highly promising to further elucidate the roles of this fascinating multisensory organ in navigation and the respective processing areas in the central brain of the ant.

ACKNOWLEDGMENTS

The authors want to thank the Greek government and the management boards of the Schinias and Strofylia National Parks for permissions to excavate ant nests. Special thanks go to Claudia Gehrig for sectioning the antennae and Sebastian Britz for introducing us to TrakEM2. The authors thank Erich Buchner and Christian Wegener for providing the anti-synapsin antibody, and Jens Habenstein and Basil el Jundi for helpful discussions on sensory projections in the central ant brain. The authors thank two reviewers for their helpful input. This study was funded by DFG grant Ro1177/7–1 and DFG equipment grant INST 93/829-1, both to WR. PNF's position is funded by DFG project FL1060/1-1 and supported by the Klaus Tschira Foundation gGmbH (project GSO/KT 16). Open Access funding enabled and organized by ProjektDEAL.

AUTHOR CONTRIBUTIONS

Robin Grob, Pauline N. Fleischmann, and Wolfgang Rössler conceived the study. Robin Grob, Claudia Groh, Christian Stigloher, and Wolfgang Rössler designed the anatomical analyzes of the JO. Robin Grob, Kornelia Grübel, Pauline N. Fleischmann, and Wolfgang Rössler designed the anterograde tracing section of the study. Robin Grob, Clara Tritscher, and Kornelia Grübel performed the experiments, collected the data and, together with Wolfgang Rössler and Pauline N. Fleischmann, analyzed and discussed the data. Wolfgang Rössler was responsible for funding acquisition for this study. Robin Grob

drafted and Wolfgang Rössler and Pauline N. Fleischmann revised the manuscript. All authors approved the final version of the manuscript for submission.

CONFLICT OF INTEREST

The authors declare no conflicts of interest.

PEER REVIEW

The peer review history for this article is available at https://publons.com/publon/10.1002/cne.25077.

DATA AVAILABILITY STATEMENT

Raw confocal, histology, scanning-electron microscopy images and 3D data are available from the authors upon reasonable request. For comparison of brain data, 3D data of the brain of Cataglyphis nodus (from Habenstein et al., 2020) are available at the Insect Brain Database website (https://www.insectbraindb.org/).

ORCID

Robin Grob https://orcid.org/0000-0002-0096-4040
Pauline N. Fleischmann https://orcid.org/0000-0002-5051-884X
Wolfgang Rössler https://orcid.org/0000-0002-5195-8214

REFERENCES

Ai, H., Nishino, H., & Itoh, T. (2007). Topographic organization of sensory afferents of Johnston's organ in the honeybee brain. *The Journal of Comparative Neurology*, *502*(6), 1030–1046. https://doi.org/10.1002/cne.21341.

Beckingham, K. M., Texada, M. J., Baker, D. A., Munjaal, R., & Armstrong, J. D. (2005). Genetics of graviperception in animals. In *Advances in genetics* (Vol. 55, pp. 105–145). Cambridge, Massachusetts, United States: Academic Press. https://doi.org/10.1016/S0065-2660(05)55004-1

Böhm, L. (1911). Die antennalen Sinnesorgane der Lepidopteren. *Arbeiten Aus Dem Zoologischen Instituten Der Universität Wien Und Der Zoologischen Station In Triest*, *2*(22), 219–246.

Boo, K. S., & Richards, A. G. (1975). Fine structure of scolopidia in Johnston's organ of female *Aedes aegypti* compared with that of the male. *Journal of Insect Physiology*, *21*(5), 1129–1139. https://doi.org/10.1016/0022-1910(75)90126-2.

Brockmann, A., & Robinson, G. E. (2007). Central projections of sensory systems involved in honey bee dance language communication. *Brain, Behavior and Evolution*, *70*(2), 125–136. https://doi.org/10.1159/000102974.

Cardona, A., Saalfeld, S., Schindelin, J., Arganda-Carreras, I., Preibisch, S., Longair, M., Tomancak, P., Hartenstein, V., & Douglas, R. J. (2012). TrakEM2 software for neural circuit reconstruction. *PLoS One*, *7*(6), e38011. https://doi.org/10.1371/journal.pone.0038011.

Cator, L. J., Arthur, B. J., Harrington, L. C., & Hoy, R. R. (2009). Harmonic convergence in the love songs of the dengue vector mosquito. *Science*, *323*(5917), 1077–1079. https://doi.org/10.1126/science.1166541.

Child, C. M. (1894). Ein bisher wenig beachtetes antennales Sinnesorgan der Insekten, mit besonderer Berücksichtigung der Culiciden und Chironomiden. *Zeitschrift für Wissenschaftliche Zoologie*, *58*, 475–528.

Currier, T. A., & Nagel, K. I. (2020). Experience- and context-dependent modulation of the invertebrate compass system. *Neuron*, *106*(1), 9–11. https://doi.org/10.1016/j.neuron.2020.03.003.

de Oliveira, J. F., Wajnberg, E., Esquivel, D. M. D. S., Weinkauf, S., Winklhofer, M., & Hanzlik, M. (2010). Ant antennae: Are they sites for magnetoreception? *Journal of the Royal Society, Interface/the Royal Society*, *7*(42), 143–152. https://doi.org/10.1098/rsif.2009.0102.

Dreller, C., & Kirchner, W. H. (1993a). How honeybees perceive the information of the dance language. *Naturwissenschaften*, *80*(7), 319–321. https://doi.org/10.1007/BF01141904.

Dreller, C., & Kirchner, W. H. (1993b). Hearing in honeybees: Localization of the auditory sense organ. *Journal of Comparative Physiology A*, *173*(3), 275–279. https://doi.org/10.1007/BF00212691.

Dreller, C., & Kirchner, W. H. (1995). The sense of hearing in honey bees. *Bee World*, *76*(1), 6–17. https://doi.org/10.1080/0005772X.1995.11099233.

Fent, K., & Wehner, R. (1985). Ocelli: a celestial compass in the desert ant *Cataglyphis*. *Science*, *228*(4696), 192–194. https://doi.org/10.1126/science.228.4696.192.

Fleischmann, P. N., Rössler, W., & Wehner, R. (2018). Early foraging life: Spatial and temporal aspects of landmark learning in the ant *Cataglyphis noda*. *Journal of Comparative Physiology A*, *204*(6), 579–592. https://doi.org/10.1007/s00359-018-1260-6.

Fleischmann, P. N., Christian, M., Müller, V. L., Rössler, W., & Wehner, R. (2016). Ontogeny of learning walks and the acquisition of landmark information in desert ants, *Cataglyphis fortis*. *Journal of Experimental Biology*, *219*, 3137–3145. https://doi.org/10.1242/jeb.140459.

Fleischmann, P. N., Grob, R., Wehner, R., & Rössler, W. (2017). Species-specific differences in the fine structure of learning walk elements in *Cataglyphis* ants. *Journal of Experimental Biology*, *220*, 2426–2435. https://doi.org/10.1242/jeb.158147.

Fleischmann, P. N., Grob, R., Müller, V. L., Wehner, R., & Rössler, W. (2018). The geomagnetic field is a compass cue in *Cataglyphis* ant navigation. *Current Biology*, *28*(9), 1440–1444. https://doi.org/10.1016/j.cub.2018.03.043.

Fleischmann, P. N., Grob, R., & Rössler, W. (2020). Magnetoreception in hymenoptera: Importance for navigation. *Animal Cognition*, *23*, 1051–1061. https://doi.org/10.1007/s10071-020-01431-x.

Göpfert, M. C., & Robert, D. (2001a). Active auditory mechanics in mosquitoes. *Proceedings of the Royal Society B: Biological Sciences*, *268*(1465), 333–339. https://doi.org/10.1098/rspb.2000.1376.

Göpfert, M. C., & Robert, D. (2001b). Turning the key on *Drosophila* audition. *Nature*, *411*(6840), 908–908. https://doi.org/10.1038/35082144.

Göpfert, M. C., & Robert, D. (2002). The mechanical basis of *Drosophila* audition. *Journal of Experimental Biology*, *205*(Pt 9), 1199–1208. http://www.ncbi.nlm.nih.gov/pubmed/11948197.

Grah, G., & Ronacher, B. (2008). Three-dimensional orientation in desert ants: Context-independent memorisation and recall of sloped path segments. *Journal of Comparative Physiology A*, *194*(6), 517–522. https://doi.org/10.1007/s00359-008-0324-4.

Grah, G., Wehner, R., & Ronacher, B. (2005). Path integration in a three-dimensional maze: Ground distance estimation keeps desert ants *Cataglyphis fortis* on course. *Journal of Experimental Biology*, *208*(21), 4005–4011. https://doi.org/10.1242/jeb.01873.

Grob, R., Fleischmann, P. N., Grübel, K., Wehner, R., & Rössler, W. (2017). The role of celestial compass information in *Cataglyphis* ants during learning walks and for neuroplasticity in the central complex and mushroom bodies. *Frontiers in Behavioral Neuroscience*, *11*, 1–14. https://doi.org/10.3389/fnbeh.2017.00226.

Grob, R., Fleischmann, P. N., & Rössler, W. (2019). Learning to navigate – How desert ants calibrate their compass systems. *Neuroforum*, *25*, 109–120. https://doi.org/10.1515/nf-2018-0011.

Guerra, P. A., Gegear, R. J., & Reppert, S. M. (2014). A magnetic compass aids monarch butterfly migration. *Nature Communications*, *5*(4164), 1–8. https://doi.org/10.1038/ncomms5164.

Habenstein, J., Amini, E., Grübel, K., el Jundi, B., & Rössler, W. (2020). The brain of *Cataglyphis* ants: Neuronal organization and visual projections. *The Journal of Comparative Neurology*, *528*, cne.24934. https://doi.org/10.1002/cne.24934.

Hallberg, E. (1981). Johnston's organ in *Neodiprion sertifer* (Insecta: Hymenoptera). *Journal of Morphology*, *167*(3), 305–312. https://doi.org/10.1002/jmor.1051670305.

Honkanen, A., Adden, A., da Silva Freitas, J., & Heinze, S. (2019). The insect central complex and the neural basis of navigational strategies. *The Journal of Experimental Biology*, *222*(Suppl 1), jeb188854. http://dx.doi.org/10.1242/jeb.188854.

Ibbotson, M. R., & Goodman, L. J. (1990). Response characteristics of four wide-field motion- sensitive descending interneurones in *Apis mellifera*. *Journal of Experimental Biology*, *148*, 255–279.

Ignell, R., Dekker, T., Ghaninia, M., & Hansson, B. S. (2005). Neuronal architecture of the mosquito deutocerebrum. *The Journal of Comparative Neurology*, *493*(2), 207–240. https://doi.org/10.1002/cne.20800.

Ishikawa, Y., Fujiwara, M., Wong, J., Ura, A., & Kamikouchi, A. (2020). Stereotyped combination of hearing and wind/gravity-sensing neurons in the Johnston's organ of *Drosophila*. *Frontiers in Physiology*, *10*, 1–8. https://doi.org/10.3389/fphys.2019.01552.

Ito, K., Shinomiya, K., Ito, M., Armstrong, J. D., Boyan, G., Hartenstein, V., … Vosshall, L. B. (2014). A systematic nomenclature for the insect brain. *Neuron*, *81*(4), 755–765. https://doi.org/10.1016/j.neuron.2013.12.017.

Johnston, C. (1855). Original communications: Auditory apparatus of the *Culex* Mosquito. *Journal of Cell Science*, *3*, 97–102.

Kamikouchi, A., Inagaki, H. K., Effertz, T., Hendrich, O., Fiala, A., Göpfert, M. C., & Ito, K. (2009). The neural basis of *Drosophila* gravity-sensing and hearing. *Nature*, *458*(7235), 165–171. https://doi.org/10.1038/nature07810.

Kamikouchi, A., Shimada, T., & Ito, K. (2006). Comprehensive classification of the auditory sensory projections in the brain of the fruit fly *Drosophila melanogaster*. *The Journal of Comparative Neurology*, *499*(3), 317–356. https://doi.org/10.1002/cne.21075.

Kirschner, S., Kleineidam, C. J., Zube, C., Rybak, J., Grünewald, B., & Rössler, W. (2006). Dual olfactory pathway in the honeybee, *Apis mellifera*. *The Journal of Comparative Neurology*, *499*, 933–952. https://doi.org/10.1002/cne.

Lucano, M. J., Cernicchiaro, G., Wajnberg, E., & Esquivel, D. M. S. (2006). Stingless bee antennae: A magnetic sensory organ? *Biometals*, *19*(3), 295–300. https://doi.org/10.1007/s10534-005-0520-4.

Markl, H. (1963). Bristle fields: Gravity receptors of some hymenoptera. *Nature*, *198*(4876), 173–175. https://doi.org/10.1038/198173a0.

Markl, H. (1962). Borstenfelder an den Gelenken als Schweresinnesorgane bei Ameisen und anderen Hymenopteren. *Zeitschrift für Vergleichende Physiologie*, *45*(5), 475–569. https://doi.org/10.1007/BF00342998.

Maronde, U. (1991). Common projection areas of antennal and visual pathways in the honeybee brain, *Apis mellifera*. *The Journal of Comparative Neurology*, *309*(3), 328–340. https://doi.org/10.1002/cne.903090304.

Masson, C., & Gabouriaut, D. (1973). Ultrastructure de l'organe de Johnston de la Fourmi *Camponotus vagus* Scop. (Hymenoptera, Formicidae). *Zeitschrift für Zellforschung und Mikroskopische Anatomie*, *140*(1), 39–75. https://doi.org/10.1007/BF00307058.

McIndoo, N. E. (1922). The auditory sense of the honey-bee. *The Journal of Comparative Neurology*, *34*(2), 173–199. https://doi.org/10.1002/cne.900340202.

McIver, S. B. (1985). Mechanoreception. In G. A. Kerkut & L. I. Gilbert (Eds.), *Comprehensive insect physiology, biochemistry, and pharmacology* (pp. 71–132). Oxford: Pergamon Press.

Mote, M. I., & Wehner, R. (1980). Functional characteristics of photoreceptors in the compound eye and ocellus of the desert ant, *Cataglyphis bicolor*. *Journal of Comparative Physiology A*, *137*(1), 63–71. https://doi.org/10.1007/BF00656918.

Okubo, T., Patella, P., D'Alessandro, I., & Wilson, R. (2020). A neural network for wind-guided compass navigation. *Neuron*, *107*, 1–17. https://doi.org/10.1016/j.neuron.2020.06.022.

Pareto, A. (1972). Die zentrale Verteilung der Fühlerafferenz bei Arbeiterinnen der Honigbiene, *Apis mellifera* L. *Zeitschrift für Zellforschung und Mikroskopische Anatomie*, *131*(1), 109–140. https://doi.org/10.1007/BF00307204.

Peeters, C., & Aron, S. (2017). Evolutionary reduction of female dispersal in *Cataglyphis* desert ants. *Biological Journal of the Linnean Society*, *122*(1), 58–70. https://doi.org/10.1093/biolinnean/blx052.

Penmetcha, B., Ogawa, Y., Ribi, W. A., & Narendra, A. (2019). Ocellar structure of African and Australian desert ants. *Journal of Comparative Physiology A*, *205*(5), 699–706. https://doi.org/10.1007/s00359-019-01357-x.

Roces, F., & Tautz, J. (2001). Ants are deaf. *The Journal of the Acoustical Society of America*, *109*(6), 3080–3082. https://doi.org/10.1121/1.1370085.

Ronacher, B. (2020). Path integration in a three-dimensional world: The case of desert ants. *Journal of Comparative Physiology A*, *206*(3), 379–387. https://doi.org/10.1007/s00359-020-01401-1.

Rössler, W. (2019). Neuroplasticity in desert ants (Hymenoptera: Formicidae) – Importance for the ontogeny of navigation. *Myrmecological News*, *29*, 1–20. https://doi.org/10.25849/myrmecol.news_029:001.

Sane, S. P., Dieudonné, A., Willis, M. A., & Daniel, T. L. (2007). Antennal mechanosensors mediate flight control in moths. *Science*, *315*(5813), 863–866. https://doi.org/10.1126/science.1133598.

Schmidt, K. (1974). Die Mechanorezeptoren im Pedicellus der Eintagsfliegen (Insecta, Ephemeroptera). *Zeitschrift Für Morphologie Der Tiere*, *78*(3), 193–220. https://doi.org/10.1007/BF00375742.

Schmitt, F., Stieb, S. M., Wehner, R., & Rössler, W. (2016). Experience-related reorganization of giant synapses in the lateral complex: Potential role in plasticity of the sky-compass pathway in the desert ant *Cataglyphis fortis*. *Developmental Neurobiology*, *76*(4), 390–404. https://doi.org/10.1002/dneu.22322.

Schmitt, F., Vanselow, J. T., Schlosser, A., Wegener, C., & Rössler, W. (2017). Neuropeptides in the desert ant *Cataglyphis fortis*: Mass spectrometric analysis, localization, and age-related changes. *The Journal of Comparative Neurology*, *525*(4), 901–918. https://doi.org/10.1002/cne.24109.

Snodgrass, R. E. (1926). The morphology of insect sense organs and the sensory nervous system. *Smithsonian Miscellaneous Collections*, *77*(8), 1–80.

Sörensen, S. P. L. (1912). Über die Messung und Bedeutung der Wasserstoffionen-konzentration bei biologischen Prozessen. *Biochemische Zeitschrift*, *12*(1), 393–532. https://doi.org/10.1007/BF02325444.

Steck, K., Hansson, B. S., & Knaden, M. (2009). Smells like home: Desert ants, *Cataglyphis fortis*, use olfactory landmarks to pinpoint the nest. *Frontiers in Zoology*, *6*, 5. https://doi.org/10.1186/1742-9994-6-5.

Stieb, S. M., Hellwig, A., Wehner, R., & Rössler, W. (2012). Visual experience affects both behavioral and neuronal aspects in the individual life history of the desert ant *Cataglyphis fortis*. *Developmental Neurobiology*, *72*(5), 729–742. https://doi.org/10.1002/dneu.20982.

Stieb, S. M., Kelber, C., Wehner, R., & Rössler, W. (2011). Antennal-lobe organization in desert ants of the genus *Cataglyphis*. *Brain, Behavior and Evolution*, *77*(3), 136–146. https://doi.org/10.1159/000326211.

Stieb, S. M., Muenz, T. S., Wehner, R., & Rössler, W. (2010). Visual experience and age affect synaptic organization in the mushroom bodies of the desert ant *Cataglyphis fortis*. *Developmental Neurobiology*, *70*(6), 408–423. https://doi.org/10.1002/dneu.20785.

Todi, S. V., Sharma, Y., & Eberl, D. F. (2004). Anatomical and molecular design of the *Drosophila* antenna as a flagellar auditory organ. *Microscopy Research and Technique*, *63*(6), 388–399. https://doi.org/10.1002/jemt.20053.

Uga, S., & Kuwabara, M. (1965). On the fine structure of the chordotonal sensillum in antenna of *Drosophila melanogaster*. *Journal of Electron Microscopy*, *14*(3), 173–181. https://doi.org/10.1093/oxfordjournals.jmicro.a049481.

Vowles, D. M. (1954). The orientation of ants: II. Orientation to light, gravity and polarized light. *Journal of Experimental Biology*, *55*, 101–114.

Wehner, R. (2003). Desert ant navigation: How miniature brains solve complex tasks. *Journal of Comparative Physiology A*, *189*(8), 579–588. https://doi.org/10.1007/s00359-003-0431-1.

Wehner, R., & Duelli, P. (1971). The spatial orientation of desert ants, *Cataglyphis bicolor*, before sunrise and after sunset. *Experientia*, *27*(11), 1364–1366. https://doi.org/10.1007/BF02136743.

Wehner, R., Meier, C., & Zollikofer, C. (2004). The ontogeny of foraging behaviour in desert ants, *Cataglyphis bicolor*. *Ecological Entomology*, *29*, 240–250. https://doi.org/10.1111/j.0307-6946.2004.00591.x.

Wehner, R. (2020). *Desert navigator*. Harvard University Press. https://doi.org/10.4159/9780674247918.

Wittlinger, M., Wehner, R., & Wolf, H. (2006). The ant odometer: Stepping on stilts and stumps. *Science*, *312*(5782), 1965–1967. https://doi.org/10.1126/science.1126912.

Wittlinger, M., Wolf, H., & Wehner, R. (2007). Hair plate mechanoreceptors associated with body segments are not necessary for three-dimensional path integration in desert ants, *Cataglyphis fortis*. *Journal of Experimental Biology*, *210*(3), 375–382. https://doi.org/10.1242/jeb.02674.

Wohlgemuth, S., Ronacher, B., & Wehner, R. (2001). Ant odometry in the third dimension. *Nature*, *411*(6839), 795–798. https://doi.org/10.1038/35081069.

Wolf, H., & Wehner, R. (2000). Pinpointing food sources: Olfactory and anemotactic orientation in desert ants, *Cataglyphis fortis*. *Journal of Experimental Biology*, *868*, 857–868.

Wystrach, A., & Schwarz, S. (2013). Ants use a predictive mechanism to compensate for passive displacements by wind. *Current Biology*, *23*(24), R1083–R1085. https://doi.org/10.1016/j.cub.2013.10.072.

Yack, J. E. (2004). The structure and function of auditory chordotonal organs in insects. *Microscopy Research and Technique*, *63*(6), 315–337. https://doi.org/10.1002/jemt.20051.

Yorozu, S., Wong, A., Fischer, B. J., Dankert, H., Kernan, M. J., Kamikouchi, A., … Anderson, D. J. (2009). Distinct sensory representations of wind and near-field sound in the *Drosophila* brain. *Nature*, *458*(7235), 201–205. https://doi.org/10.1038/nature07843.

How to cite this article: Grob R, Tritscher C, Grübel K, et al. Johnston's organ and its central projections in *Cataglyphis* desert ants. *J Comp Neurol*. 2021;529:2138–2155. https://doi.org/10.1002/cne.25077